

Article

Arginine-Vasotocin Neuronal System in *Steindachneridion parahybae* (Siluriformes: Pimelodidae) and Its Influence on Artificially Induced Spawning in Captivity

Renato M. Honji ^{1,*}, Bruno C. Araújo ², Paulo H. de Mello ³, Martín R. Ramallo ⁴, Leonel Morandini ⁴, Danilo Caneppele ⁵ and Renata G. Moreira ⁶

¹ Laboratório de Aquicultura e Ecofisiologia Marinha (LAQUEFIM), Departamento de Fisiologia, Instituto de Biociências, Universidade de São Paulo (IB/USP), Rua do Matão, Travessa 14, nº 321, São Paulo 05508-090, SP, Brazil

² Núcleo Integrado de Biotecnologia, Universidade de Mogi das Cruzes, Mogi das Cruzes 08701-970, SP, Brazil

³ Beacon Development, King Abdullah University of Science and Technology, Thuwal 23955-6900, Saudi Arabia

⁴ Departamento de Biodiversidad y Biología Experimental, Facultad de Ciencias Exactas y Naturales, Universidad de Buenos Aires & IBBEA, CONICET/UBA, Ciudad Universitaria (C1428EHA), Buenos Aires 5000, Argentina

⁵ HMZ Aquicultura & Conservação. Rua Telmo Arnaut de Carvalho, 262, Paraibuna 12260-000, SP, Brazil

⁶ Laboratório de Metabolismo e Reprodução de Organismos Aquáticos (LAMEROA), Departamento de Fisiologia, Instituto de Biociências, Universidade de São Paulo (IB/USP), Rua do Matão, Travessa 14, nº 321, São Paulo 05508-090, SP, Brazil

* Correspondence: honjijp@usp.br



Citation: Honji, R.M.; Araújo, B.C.; de Mello, P.H.; Ramallo, M.R.; Morandini, L.; Caneppele, D.; Moreira, R.G. Arginine-Vasotocin Neuronal System in *Steindachneridion parahybae* (Siluriformes: Pimelodidae) and Its Influence on Artificially Induced Spawning in Captivity. *Fishes* **2024**, *9*, 235. <https://doi.org/10.3390/fishes9060235>

Academic Editor: José

A. Muñoz-Cueto

Received: 15 April 2024

Revised: 6 June 2024

Accepted: 15 June 2024

Published: 18 June 2024



Copyright: © 2024 by the authors. Licensee MDPI, Basel, Switzerland. This article is an open access article distributed under the terms and conditions of the Creative Commons Attribution (CC BY) license (<https://creativecommons.org/licenses/by/4.0/>).

Abstract: This study summarizes new data on induced spawning of *Steindachneridion parahybae*, focusing on the aggressive behavior of females. This study characterizes the vasotocinergic system using immunohistochemistry, highlighting the potential influence of arginine-vasotocin (AVT) on reproductive physiology. Two experimental groups were proposed: (A) control, with one female in the aquarium, and (B) experimental, with two females in the same aquarium. Dominant (D) females presented a more aggressive behavior and did not show any injury. They apparently had a length and body mass higher than injured nondominant (ND) females. The analysis identified positive AVT immunoreactive (ir) neurons exclusively within the preoptic area, including parvocellular, magnocellular, and gigantocellular subpopulations, containing fibers-ir extending into the pituitary gland. Cellular and nuclear areas were greater in D compared to ND in the magnocellular subpopulation. There were no differences between parvocellular and gigantocellular subpopulations. There was a difference on the steroid plasma profile of cortisol (more in ND than in D) and 17 α ,20 β -dihydroxy-4-pregnen-3-one (more in D than in ND). Furthermore, control and D females presented higher optical densities for AVT-ir, gonadotropin-releasing hormone-ir, and luteinizing hormone-ir than ND. In general, there were no differences in the results of female (control group) with D females. The AVT system is highly complex, possibly counting multiple sites of action during artificial reproduction and acting directly and/or indirectly associated with behavioral and physiological changes in *S. parahybae* females when induced to spawning.

Keywords: reproduction; neuroendocrinology; sexual steroid; agonistic behavior; aggression

Key Contribution: This is the first study characterizing the vasotocinergic system and its influence on social behavior and reproductive physiology of females of an endangered Neotropical catfish (*Steindachneridion parahybae*) during induction to breeding in captivity. Dominant females show better reproductive results and lower plasma cortisol concentrations than nondominant females. There are also greater optical densities of the following neurohormones: gonadotropin-releasing hormone and arginine-vasotocin, and the pituitary hormone β -luteinizing hormone. The current results suggest possible effects of the arginine-vasotocin system on aggressive behavior and steroidogenesis.

1. Introduction

Steindachneridion parahybae (Steindachner, 1877) is a medium-sized Neotropical catfish species that is endemic to the Paraíba do Sul River basin in Brazil [1]. It is listed in the “Brazil Red Book of Threatened Species of Fauna” and on the “International Union for Conservation of Nature’s Red List of Threatened Species” (IUCN), both as “endangered species” [1,2]. There are no reports of this species in the southern rivers of the Paraíba do Sul River basin [1]. Nevertheless, *S. parahybae* had been commonly captured in commercial fisheries along the Paraíba do Sul River basin during the 1950s (around 1000 kg/year) [1]. Over the last few years, a conservation action has promoted a fish restocking program coordinated by the former Companhia Energética de São Paulo (CESP). This company had supported research on the biology of *S. parahybae*, especially on reproductive physiology and development biology. Studies on *S. parahybae* aimed mainly to establish of a protocol for artificial spawning [3,4], develop embryos and larvae [5–7], improve broodstock metabolism [8] and the neuroendocrine system [9–11], and improve the quality of gametes of *S. parahybae* [6,11–13].

The key component regulating fish reproduction is the neuroendocrine system, primarily through the brain-pituitary-gonadal (BPG) axis (see: [14–18] for review). Studies on the neural and hormonal processes that control the BPG axis of *S. parahybae* have sought to analyze the artificial reproduction and describe that the impediment of *S. parahybae* reproductive migration via natural or human interference changes the reproduction physiology of this species [3,9–11]. These previous studies on *S. parahybae* females in captivity revealed that rearing broodstocks of this species was not entirely successful due to observed reproductive dysfunction. This dysfunction includes failure to undergo final oocyte maturation (FOM), ovulation, and spawning, suggesting the presence of endocrine dysfunction in these animals when raised in captivity. The absence of FOM and ovulation in *S. parahybae* females suggests a disruption in the synthesis and/or release of LH and/or the GnRH system [9–11]. On the other hand, *S. parahybae* males do not present any reproductive dysfunction when kept in captivity, they complete spermatogenesis naturally (sometimes there is a need for artificial induction with exogenous hormones just to increase the semen released during induced reproduction) [12,13]. In addition, the maintenance of *S. parahybae* females in captivity suggests that these animals undergo multiple spawning events during the reproductive cycle [9–11]. Nevertheless, due to the scarcity of animals in the natural environment, it is hard to understand the reproductive biology of *S. parahybae*. Furthermore, during the first attempt at artificial induction to spawning of wild *S. parahybae* in captivity, after 200 ATUs (accumulated thermal units) and under an average temperature of 24 °C, it is possible to observe an increase in the animal’s activity, including an aggressive behavior of females that harms the partner (males), forcing the separation of the animals in this first attempt, and not maintaining wild animals at risk [3]. Continuing the attempts to induce reproduction of *S. parahybae* in captivity and adjust the induction protocol, Honji et al. [4] observed such behavior and described the aggressive behavior between two females after the second hormone dose until the gamete’s dry extrusion, allowing us to ask/hypothesize several questions about the aggressive behavior of *S. parahybae* females in captivity during artificial reproduction.

Several groups of neurohormones are involved in mediating social and reproductive behavior via interactions with other neuropeptides or neurotransmitter systems in the fish brain, including alternative phenotypes (variation in social dominance or the control of a territory) and/or social cognition (interactions) [19–23]. Among these neuropeptides, the vasopressin-vasotocin peptide family modulates several processes in reproductive physiology, comprising both aggressive and reproductive behaviors [19,24,25]. The non-peptide arginine-vasotocin (AVT) in nonmammals and its mammalian homolog arginine-vasopressin (AVP) is expressed in the brain and affects numerous social behaviors by acting in the BPG axis [20,26,27]. In fish, the vast majority of studies only examined AVT in males, mainly in relation to social behaviors (establishment of dominance hierarchy) [19,20,24], separating males by reproductive or social status while females were grouped into a single category. However, it is also important to examine plasticity of the AVT system in

female fish; they also undergo cyclical changes in behaviors and reproductive physiology, comparable to males, in many species, especially in those where males do not present social hierarchies (and no reproductive dysfunction in captivity) instead of females, when they are very aggressive and also show reproductive dysfunction in captivity, as with *S. parahybae*. Additionally, neurohormones and sexual steroids maintain and regulate AVT synthesis in the fish brain, suggesting that reproductive status regulates the AVT system [24–27]. Therefore, it is recommended to analyze the AVT system in males and females separately. In this context, research has linked AVT to stress responses because of AVT neurons via innervate corticotroph cells of the pituitary gland. It affects adrenocorticotropin (ACTH) release and thus cortisol secretion from the interrenal gland [28]. It also affects sexual plasticity, such as regulating behavioral sex change [29], and social behavior, such as dominant/subordinate behavior [19,22,25,30], courtship [31], aggression [25,32], among others [20,26,29,33]. Therefore, the AVT peptide also provides an integrational neural substrate for a dynamic modulation of these behaviors by promoting endocrine and sensory stimuli [20,25,33].

Nonapeptide AVTs are found predominantly in three different cell populations within a preoptic area (POA) located in the anterior hypothalamus (see: [24,26,34–36] for review). Subpopulations of cells in POA can associate with different functions, including stress response, territorial behavior, among others. Nevertheless, little is known about the potential physiological roles of AVT system in Neotropical fish or the relation of AVT neurons to other neuroendocrine circuits controlling reproduction. This possible relationship may be species-specific. Data on the AVT neuronal system (present study), gonadotropin-releasing-hormone system [10], gonadotropins and growth hormone family members [9], steroid synthesis pathways, and oocyte development [11] must be interpreted together in order to solve the puzzle of the reproductive dysfunction of captive *S. parahybae* females, especially improving the understanding of their reproductive physiology since the endangered status of the species deserves special attention and urgent actions. Therefore, this study aimed to characterize the vasotocinergic system of *S. parahybae* during artificially induced spawning, focusing on the reproductive behavior of females. Then, after characterizing this system, we related AVT across the BPG axis, and its effects on reproductive dysfunction of captive *S. parahybae* broodstock (F1). Using immunohistochemistry and morphometry of AVT neurons as proxies, we predicted that AVT influences the BPG axis, affecting reproductive performance and behavior of *S. parahybae* females.

2. Materials and Methods

The present study was conducted at the *Unidade de Hidrobiologia e Aquicultura da CESP de São Paulo* (23°41'39" S and 45°60'42" W), located in the municipality of Paraibuna (São Paulo State, Brazil). *S. parahybae* females (F1) were obtained via artificially induced reproduction with wild broodstocks at the same station [3]. In December 2007, a hundred adults of *S. parahybae* females, born and raised at CESP, were kept into two earth ponds (200 m²). Fish were fed at 8 am and 4 pm on commercially extruded food for carnivorous fish, containing 40% of crude protein, at a rate of 2% biomass/day, offered twice a day (according to CESP's fish farm routine). The annual mean water temperature and dissolved oxygen concentration (monitored with an oximeter, Horiba-ModU10) were 21.10 ± 0.14 °C and 7.58 ± 0.36 mg/L, respectively.

2.1. Broodstock Selection, Hormonal Induction, Reproductive Behavior, and Spawning

Steindachneridion parahybae females born and raised at CESP fish farm were selected based on the typical morphological characteristics of sexual maturity, according to parameters previously established for this species [3–5]. Captivity females (Table 1) were selected via external characteristics according to the hyperemic genital pore and the swollen abdomen. A biopsy was performed in these females, cannulating the gonoduct with a fine polyethylene catheter (5 mm external diameter) attached to a plastic syringe through the urogenital papilla. After this procedure, several oocytes were collected to examine

their size, appearance, and diameter homogeneity. These are important criteria to establish the spawning readiness of the female broodstock in artificial hormonal induction [5]. The homogeneity of oocyte diameter was analyzed with a stereomicroscope (Leica S9D stereomicroscope, Leica MC170HD photographic camera, and computer image capture, Leica LAS Interactive Measurements). Wild males (Table 1) were chosen according to the white color and the high fluidity of milt, after massaging gently the abdominal region.

Table 1. Data on *Steindachneridion parahybae* reproduction at the *Unidade de Hidrobiologia e Aquicultura da Companhia Energética de São Paulo* during their reproductive period. The broodstock's biometrical parameters (total length and weight), temperature (°C), and dissolved oxygen (mgL^{-1}) of water are shown. Data are presented as the mean \pm mean standard error ($M \pm \text{MSE}$).

Animal	<i>n</i>	Total Length (cm)	Total Weight (g)	hCG (IU/kg)	First CPE Dose (mg/kg)	Second CPE Dose (mg/kg)
Females	9	38.92 \pm 1.39	612.78 \pm 17.33	2	0.5	5
Males	3	43.00 \pm 2.08	1575.00 \pm 75.00	-	-	3
First injection (0.5 mg cPE per kg^{-1})					24.6 °C and 7.74 mgL^{-1}	
Second injection (5.0 mg cPE per kg^{-1})					23.9 °C and 8.14 mgL^{-1}	
Spawning					25.0 °C and 8.20 mgL^{-1}	

The selected broodstocks ($n = 9$) in the earth ponds were transferred to the CESP laboratory and kept in aquaria (1000-L tanks). Next, females were weighed and immediately induced to reproduce by combining whole acetone-dried carp pituitary extract (cPE) and human chorionic gonadotropin (hCG) as below [3–5]. Two doses (0.5 and 5.0 mg cPE per kg^{-1} of fish body weight dissolved in 0.9% sodium chloride solution) were considered for females within a 12 h interval between cPE doses. The hCG concentration was 2 IU per kg^{-1} for females. This dose was applied only when the second dose was administered. For males, a single dose was given at the same time as the females' second dose. This dose contained 3 mg cPE per kg^{-1} of fish body weight dissolved in 0.9% sodium chloride solution. Table 1 shows a summary of the doses used in this protocol (plus the average water temperature and dissolved oxygen concentration during the females' first and second doses).

After hormone administration up to spawning, two female broodstocks (experimental group, $n = 2/\text{aquarium}$) were placed together in a glass aquarium at the CESP laboratory in triplicate ($n = 6$) to facilitate the observation of reproductive behavior during artificial induction (Figure 1a,b). Males were kept together in a single tank outside at the CESP laboratory. Their behavior was not analyzed because males do not show aggressive behaviors (between them either before or after hormonal induction). The control group ($n = 1/\text{aquarium}$, in triplicate $n = 3$) counted only one female in each glass aquarium (Figure 1c). Following the final hormonal induction, the female gametes were placed in dry plastic containers after abdominal massage performed from head to tail (manually stripping). The semen was collected in the same way, mixed with oocytes, and homogenized. Fertilization was performed by gently mixing the gametes (routine "dry" method), followed by adding water to trigger fertilization. The eggs were transferred to 200-L conical incubators. Water temperature and dissolved oxygen concentrations were registered (Table 1).

Approximately six/eight hours after the eggs were placed in the conical incubator and after the gastrula stage established [5], the fertility rate was calculated according to the equation $F = (\text{number of fertilized eggs} \times 100) / \text{number of total eggs}$. This protocol derives from a routine adopted at the CESP [3–5]. Fertilized eggs were distinguished from unfertilized eggs according to general aspect and color and considering that unfertilized eggs are opaque.



Figure 1. (a) Aggressive behavior between *Steindachneridion parahybae* females when kept in the same aquarium during the artificial spawning in captivity (CESP collection images); (b,c) schematic drawing showing the experimental design: (b) two *S. parahybae* females in the same aquarium; and (c) control group, one *S. parahybae* female in the aquarium. Broodstock female, 635 g (total body mass), Paraíba do Sul River basin, Paraíba, São Paulo State, Brazil.

2.2. Fish Collection to Steroid Analysis, Ovarian Histological Analysis, and Brain and Pituitary Gland Histological and Immunohistochemical Analysis

Following gamete extrusion and shortly after females were manually stripped for gamete collection, all females were sampled immediately (control and experimental group). The wild male broodstocks were transferred back into their original ponds (100% survival). It is relevant to highlight that *S. parahybae* males were extensively studied (gamete quality) by Okawara et al. [7], and Sanches et al. [12,13]. Seminal quality did not limit the procedures in the present study. All females were anesthetized with 0.1% benzocaine (ethyl-p-aminobenzoate). Total and standard length (cm) and total body weight (g) were recorded. Next, blood samples were taken by a puncture in the caudal vein using a heparinized syringe. The collected blood was centrifuged for 5 min at 655.1 g. The obtained plasma was frozen and kept at -80°C until steroid analysis. Then, the fish were euthanized by decapitation at the level of the operculum. The ovaries were removed, and the brain and the pituitary (Pi) gland were collected via careful head removal and fixed in Bouin's solution for 24 h.

2.2.1. Steroid Analysis

Plasma levels of cortisol (Cort), 17β -estradiol (E_2), testosterone (T), 11-ketotestosterone (11-KT), and 17α -20 β -dihydroxy-4-pregnen-3-one (17α -20 β -DHP) of all *S. parahybae* females were quantified via hormone enzyme-linked immunosorbent assays (ELISA) using commercial kits (Cayman Chemical Company, Ann Arbor, MI, USA, for 11-KT and 17α -20 β -DHP; IBL International, Hamburg, Germany, for Cort, E_2 and T). Analyses were conducted according to the manufacturer's instruction. Absorbance measurements were performed with a microplate reader (Molecular Devices, SpectraMax 250, Sunnyvale, CA, USA). Honji et al. [11] validated the assays of E_2 , T, 11-KT, and 17α -20 β -DHP previously. Cortisol assay was validated using the same method, the detection limit was 2.46 ng/mL for Cort. Working dilutions were 1:2 to 1:8 for Cort. Intra- and inter-assay coefficients of variation (CVs) were (minimum-maximum) 0.50–8.50% and 1.79–19.67% for Cort. The acceptable limit for the intra- and inter-assay %CV was ≤ 20.0 (according to our previous studies).

2.2.2. Ovarian, Brain, and Pituitary Gland Histological Analysis

After fixing the sampled tissues in Bouin's solution, they were dehydrated using a series of increasing ethanol concentrations. The samples were then cleared with dimethylbenzene solution and embedded in Paraplast[®] according to routine histological procedures. Ovary sections (5 μm thick) and brain and Pi (12 μm thick) serial sections were obtained using a microtome (Leica HistoCore AutoCut, Deer Park, IL, USA) mounted on Poly-L-Lysine solution-coated slides. Ovary tissues were stained with haematoxylin and eosin to characterize ovary histology. Brain and Pi samples were stained with acid haematoxylin, PAS, and Masson's trichrome to precisely locate the various brain and nucleus areas and Pi regions.

The sections were mounted in Erv-Mount[®] and then examined and documented using a computerized image analyzer (Leica DM1000 LED light microscope, Leica MC170HD photographic camera, and computer image capture, Leica LAS Interactive Measurements, Deer Park, IL, USA). To identify precisely the different oocyte development stages and distinct subdivisions (neurohypophysis and adenohypophysis) and pituitary cells of *S. parahybae*, this study used the detailed description of ovarian maturation stages described by Honji et al. [11] and pituitary gland characterization described by Honji et al. [9]. Furthermore, to precisely locate the various brain and nucleus areas, this study consulted detailed previously published atlases of other species, namely sea bass (*Dicentrarchus labrax*) [37–39], zebrafish (*Danio rerio*) [40], African catfish (*Clarias gariepinus*) [41,42], medaka (*Oryzias latipes*) [43], and an atlas currently under production for *S. parahybae* (Honji et al., in preparation).

2.2.3. Single Immunohistochemistry of the Brain and Pituitary Gland

Immunohistochemistry (IHC) analyses used brain and Pi gland sections. Sections were immunostained using the Catalyzed Signal Amplification System (CSA Amplification System Kit-Code: K1500, Dako kit), following the manufacturer's instructions. The samples were deparaffinized with dimethylbenzene, rehydrated via different graded ethanol concentrations (absolute, 96, 90, and 70%), then washed with PBS buffer (phosphate buffered saline, pH 7.4), and treated with 0.3% hydrogen peroxide (H₂O₂) in PBS for 15 min at room temperature (rt) to block endogenous peroxidase activity. Then, samples were washed again with PBS and treated with 5% nonfat dry milk in PBS buffer for 30 min at rt to inactivate nonspecific sites (blocking solution). Next, sections were incubated overnight at 4 °C with a 1:500 dilution of primary rabbit antiserum (rabbits were injected with an AVT Synpep coupled to Keyhole Limpet Hemocyanin). After incubation with the primary antibody, the sections were washed in PBS buffer for 5 min (rt) and then incubated for 45 min (rt) with a biotinylated secondary antibody (Sigma-Aldrich, St. Louis, MO, USA, anti-rabbit, IgG, diluted 1:600). In order to amplify the signal, the sections were washed in PBS buffer (5 min at rt) and then sequentially incubated in streptavidin, tyramide and peroxidase-conjugated streptavidin solutions (CSA Amplification System Kit, Dako) for 45 min at rt. Finally, the samples were washed with PBS buffer. Peroxidase activity was visualized using 3,3'-diaminobenzidine (DAB) in a chromogen solution and DAB substrate buffer. Subsequently, the sections were lightly counter-stained with acid haematoxylin for 2 to 3 min, mounted in Erv-Mount[®], and analyzed using computerized image analysis (as described above).

To confirm the specificity of IHC reactions with heterologous antisera against AVT in the brain and pituitary gland of *S. parahybae*, the procedures adopted were preadsorption tests and control assays. Control sections were incubated with the primary antibody preadsorbed with excess AVT (1 µg/mL) (Sigma-Aldrich [Arg8]-vasotocin acetate salt, St. Louis, MO, USA), as previously performed with other species, such as *chanchita* (*Cichlasoma dimerus*) [30]. To avoid false positive reactions, the primary antibody was replaced with PBS or normal biotinylated secondary antibody (in place of primary antibody). There were no positive structures or cells in these sections (Figure 2a,b). The IHC analyses for gonadotropin-releasing hormone (GnRH1 or cfGnRH—catfish GnRH; dilution to primary antibody African catfish (*C. gariepinus*) 1:500; secondary antibody anti-rabbit 1:600; GnRH2 or cGnRH-II—chicken-II GnRH; dilution to primary antibody sea bass (*D. labrax*) 1:500; secondary antibody anti-guinea pig 1:600) and β -luteinizing hormone (β -LH; dilution to primary antibody mummichog (*Fundulus heteroclitus*) 1:1,000; secondary antibody anti-rabbit 1:600) were carried out in accordance with previous studies of the research group of the present authors [9,10], including specificity of IHC reactions with heterologous antisera. For this reason, GnRH and LH analyses of *S. parahybae* are not presented in this study's results, especially regarding histological description and regions where species were identified, as the study group has already published these results. Further details can be found in the mentioned studies [9,10]. Histological slides were deposited in the collection of the Laboratório de Aquicultura e Ecofisiologia Marinha (LAQUEFIM), Instituto de Biociências, Universidade de São Paulo, Brazil.

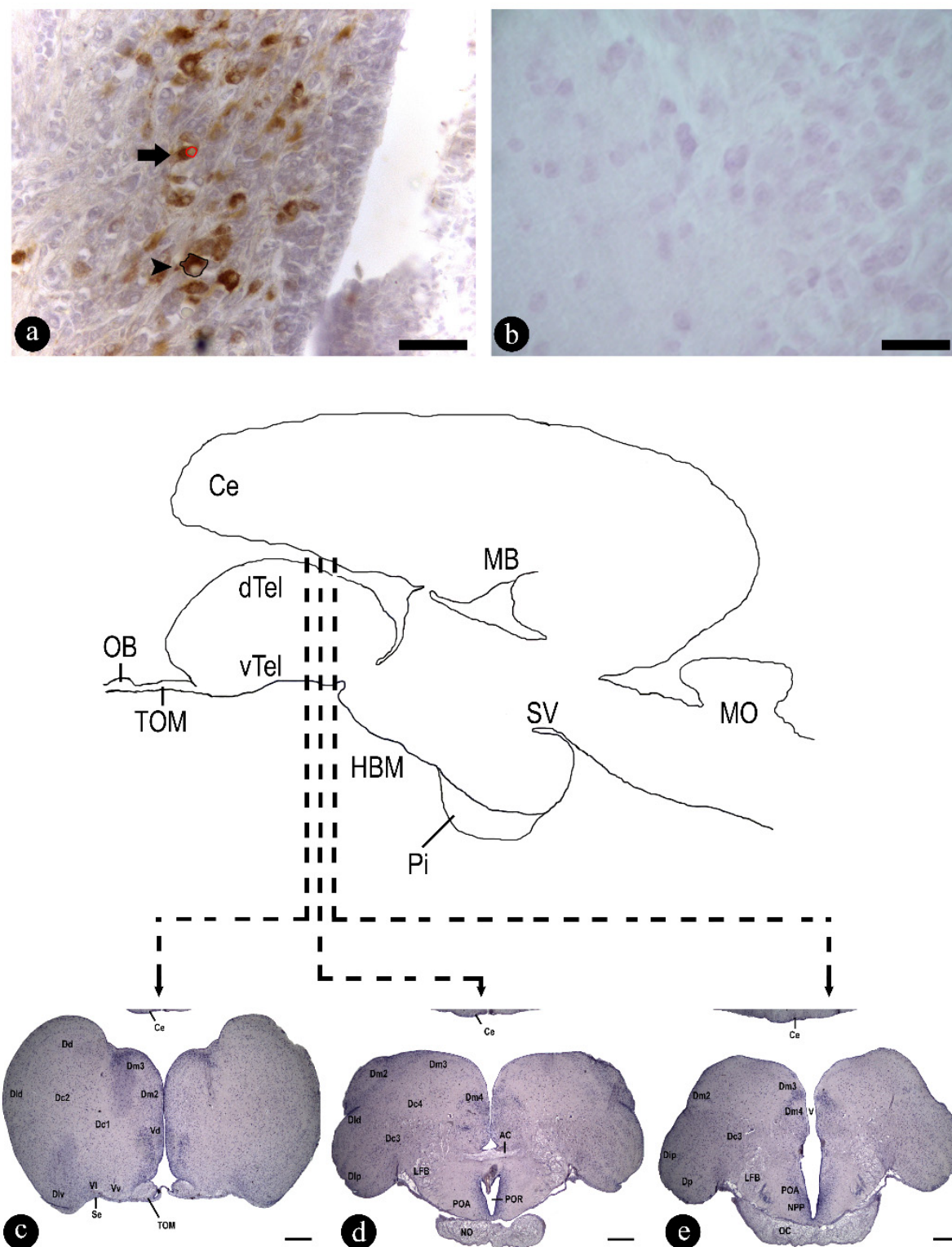


Figure 2. (a,b) Transversal sections through the preoptic area (POA) of *Steindachneridion parahybae* brain: (a) Arginine vasotocin (AVT) antiserum specificity was tested via antiserum alone; and (b) by preadsorption with an excess of antigen on successive 12 µm sections. Photomicrograph of the stained (immunostaining) with AVT neurons: (a) example of measured cellular area (black circle, arrowhead) and nuclear area (red circle, arrow); (c–e) lettered lines indicate the levels of the main nucleus of the transverse sections of the anterior (c) to the posterior (e) region of POA (preoptic area), and (c) telencephalic region and their nuclei; (d,e) preoptic area and their key nuclei. AC, anterior commissure; Ce, cerebellum; Dc1, central part of the dorsal telencephalon, subdivision 1; Dc2, central part of the dorsal telencephalon, subdivision 2; Dc3, central part of the dorsal telencephalon,

subdivision 3; Dc4, central part of the dorsal telencephalon, subdivision 4; Dp, posterior part of the dorsal telencephalon; LFB, lateral forebrain bundle; NO, optic nerve; NPP, nucleus preopticus periventricularis; OC, optic chiasma; POA, preoptic area; POR, preoptic recess; Se, sulcus externus; TOM, medial olfactory tract; V, ventricle; Vd, dorsal nucleus of the ventral telencephalon; Vl, lateral nucleus of the ventral telencephalon; Vv, ventral nucleus of the ventral telencephalon. Transversal sections of pituitary and brain stained using acid haematoxylin (central area) (adapted from Honji et al. [10]). Ce, cerebellum; dTEL, dorsal telencephalon; HBM, medial basal hypothalamus; MB, midbrain; MO, medulla oblongata; OB, olfactory bulb; Pi, pituitary gland; SV, saccus vasculosus; TOM, medial olfactory tract; vTEL, ventral telencephalon. Scale bar: 10 μm (a,b); 400 μm (c–e).

2.2.4. Morphometric Analysis

The morphometrical analysis of AVT immunoreactive (-ir), cfGnRH-ir, cGnRH-II-ir, and β -LH-ir of *S. parahybae* during artificially induced spawning in captivity, the following parameters were considered: cellular and nuclear areas (μm^2), and optical density (OD) of immunostaining (a.u.). For these analyses, images captured for each sample (ten images per animal) using the LAS system (1260 \times 960 pixels) were considered. As cell bodies are irregular in shape and most split during histological section, this study only analyzed cells in which the nucleus was clearly visible. Ten AVT ir-neurons, eight cfGnRH and cGnRH-II ir-neurons, and fifteen β -LH ir-cells were analyzed as for cellular and nuclear areas (per animal) (Figure 2a represents an example of analysis to AVT-ir neurons) using the software Leica LAS Interactive Measurements. To analyze the OD of immunostaining, the same images above were analyzed with the software Image Gauge. As well as for the measurements of the cell bodies, ten AVT ir-neurons, eight cfGnRH and cGnRH-II ir-neurons, and fifteen β -LH ir-cells were analyzed for OD of immunostaining (based only on neurons and/or cells that were immunoreactive). Additionally, to reduce variability in the results of immunostain intensity between tissues, processed separately, representatives of brain and Pi samples were included in each batch of IHC reactions to further control staining differences. Similar analyses have been performed of other teleost species [44–47], including a study examining *S. parahybae* pituitary cells (β -LH-ir) and neurons (cfGnRH-ir and cGnRH-II-ir) [9,10].

2.3. Statistical Analyses

A descriptive analysis was performed, and all values are expressed as mean \pm mean standard error (M \pm MSE). The assumptions (homogeneity and normality) were previously verified (Levene's test). In this context, if data fit a Gaussian distribution (normal distribution), they were analyzed via parametric test, otherwise, nonparametric comparisons were performed when data did not conform to the assumption of homogeneous variances. Biometrical parameters, steroid plasma levels, and morphometric data were compared via one-way analysis of variance (ANOVA) between experimental groups, followed by post hoc Tukey test (parametric comparisons). If data were nonparametric, a Kruskal–Wallis test, followed by Dunn's test was performed. Statistical differences were significant when $p < 0.05$. Additionally, Pearson's correlation analysis was conducted to ascertain the linear relationship between measurements. It assigned a value ranging from -1 to 1 , where 0 indicates no correlation, 1 represents perfect positive correlation, and -1 denotes perfect negative correlation. Additionally, a 5% confidence level (interval) was considered. All statistical analyses were performed using the statistical software SigmaStat for Windows (version 3.10; Systat Software, San Jose, CA, USA).

3. Results

3.1. Water Quality

Table 1 shows water quality parameters recorded throughout the experiment. The average water temperature and oxygen concentration during the first and second doses were 24.6°C and 7.74 mgL^{-1} , and 23.9°C and 8.14 mgL^{-1} , respectively. The average water temperature and oxygen concentration during spawning were 25.0°C and 8.20 mgL^{-1} .

3.2. Broodstock Selection, Hormonal Induction, Reproductive Behavior, and Spawning

Mature *S. parahybae* broodstocks (Table 1) appeared in February and could spawn. All broodstocks (100% survival) induced to spawning with the specific protocol described here responded positively to artificial reproduction. Captivity females were smaller than wild males (Table 1). It was not possible to establish the age of males because they were all wild specimens. However, all animals were adults and consequently older than the captivity females.

In the experimental group, after the first dose until the second hormonal dose (12 h of interval between doses), female broodstocks were not active and did not show aggressive interactions, only occasional sporadic active movements. After the second hormonal dose, there was a gradual increase in the animals' activity (qualitative analysis), including aggressive behavior that even hurt one of the females. A female chased the other, trapped it in a corner of the aquarium. Sometimes the chasing specimen had physical contact with other females, including biting and tail-hitting them. At the time of manually stripping for gamete collection, one female was damaged and the other had no injuries in the experimental aquariums. In this case, females who showed a more aggressive behavior apparently had a longer length and higher body mass than injured females (not statistically significant) (Table 2). Based on this information, this study defined as "dominant" females (D) those presenting a more aggressive behavior with no injuries and as "nondominant" females (ND) those that were injured (Table 2). Such injuries appeared throughout the body of the ND female, including the dorsal part of the body and the caudal fin. Therefore, in the present study, aggressive behavior was based on the physical attacks that ND females suffered but was not quantified during the hormonal induction process.

Table 2. Reproductive data in control, dominant and nondominant *Steindachneridion parahybae* female at the Unidade de Hidrobiologia e Aquicultura da Companhia Energética de São Paulo (CESP). Broodstocks biometrical parameters (total length and weight); total oocytes spawned weight; oocytes per spawned grams; rough estimate of oocytes per kg of female; and total fertilization rate. Data are presented as the mean \pm mean standard error (M \pm MSE).

Animal	n	Total Length (cm)	Total Weight (g)	Total Oocytes Spawned Weight (g)	Oocytes/Grams Spawned	Oocytes/kg of Female
Females (control)	3	38.92 \pm 0.52	633.33 \pm 18.78	29.90	295.87 \pm 14.56	~5523
Females (Dominant)	3	39.43 \pm 0.41	626.67 \pm 35.28	30.80	298.67 \pm 10.48	~5125
Females (Nondominant)	3	38.40 \pm 0.59	598.33 \pm 15.90	19.40	294.29 \pm 18.99	~3225
Total fertilization rate (%)		31.50 \pm 10.20% (control); 27.20 \pm 18.70% (dominant); 21.50 \pm 10.00% (nondominant)				

Spawning occurred at 200 and 220 ATU (at 25 °C). The total spawned egg weight was 80.10 g and the fertilization rate was 31.50 \pm 10.20% for the control group, 27.20 \pm 18.70% for the D group, and 21.50 \pm 10.00% for the ND group (Table 2). D and ND females spawned 30.80 g and 19.40 g of eggs, respectively, containing 298.67 \pm 10.48 oocytes/gram. D females produced approximately 5,125 oocytes/kg containing 294.29 \pm 18.99 oocytes/gram, and ND females produced approximately 3225 oocytes/kg (Table 2). In the control group, females spawned 29.90 g containing 295.87 \pm 14.56 oocytes/gram, producing approximately 5523 oocytes/kg.

3.3. Steroid Analysis

ND females had plasma Cort levels approximately 4.3 times higher than D females and 4.2 times than control females (326.14 \pm 13.18, 76.04 \pm 3.98, and 77.65 \pm 1.55 ng/mL, respectively, $p \leq 0.001$) (Figure 3a). Plasma E₂, T, and 11-KT levels of all females (ND, D, and control) were not statically different (E₂: 845.03 \pm 228.78, 853.17 \pm 126.09, and 819.35 \pm 119.87 pg/mL, $p = 0.989$; T: 0.59 \pm 0.27, 0.46 \pm 0.13, and 0.49 \pm 0.06 ng/mL, $p = 0.886$; 11-KT: 28.03 \pm 8.25, 9.10 \pm 1.43, and 13.36 \pm 2.54 pg/mL $p = 0.363$) (Figure 3b–d). Contrary to Cort levels, D and control females showed 17 α -20 β -DHP levels higher than

ND females (~2.10 times higher in relation to D and ~1.99 higher in relation to the control): $31,889.63 \pm 1369.23$ (D), $33,782.16 \pm 1804.23$ (control), and $16,052.62 \pm 1,651.38$ pg/mL (ND) ($p \leq 0.001$) (Figure 3e).

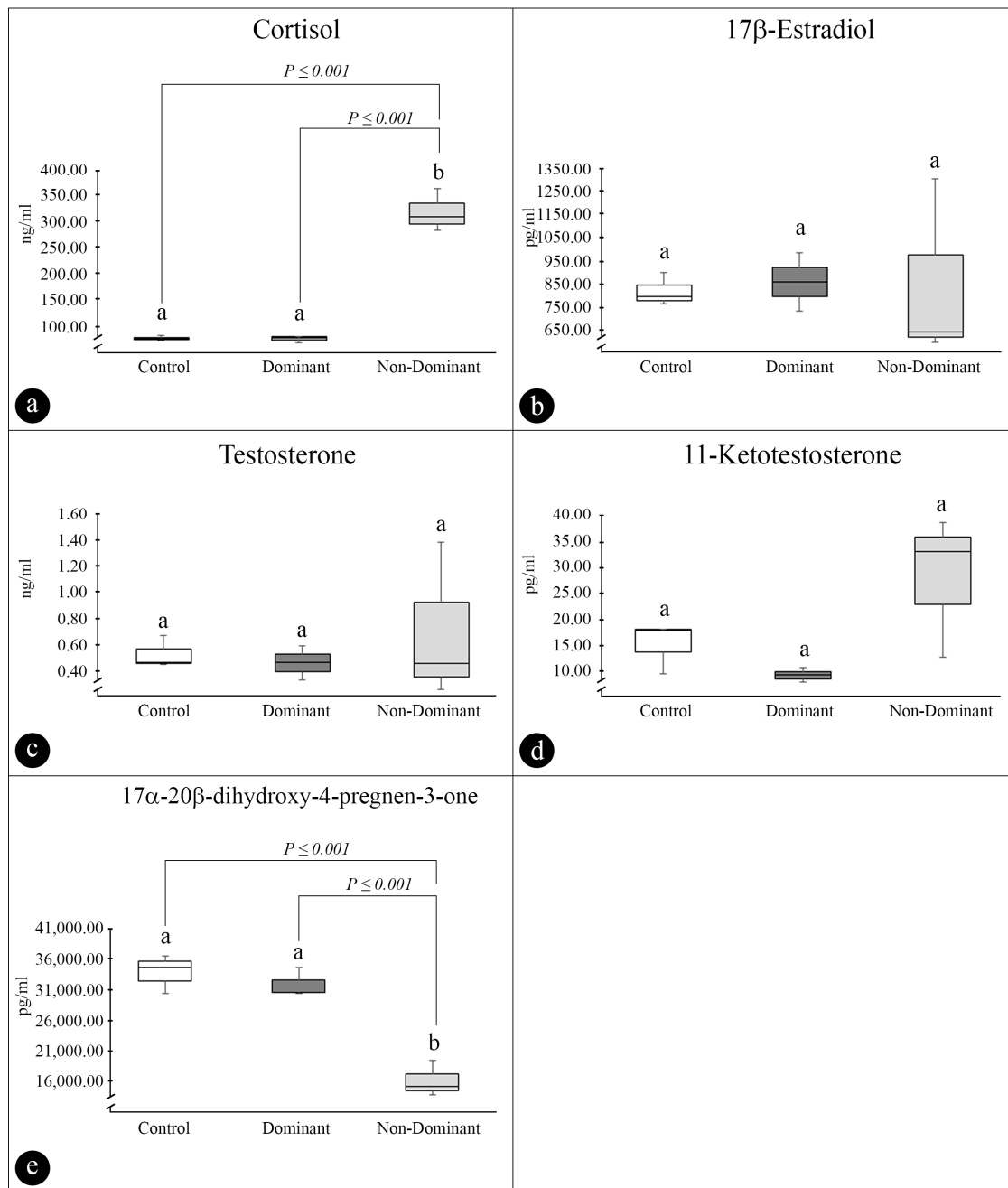


Figure 3. (a–e) Plasma sex steroid levels in control, dominant and nondominant *Steindachneridion parahybae* females during artificial spawning in captivity. (a) Plasma cortisol (Cort); (b) plasma 17β-Estradiol (E2); (c) plasma testosterone (T); (d) plasma 11-ketotestosterone (11-KT); and (e) plasma 17α,20β-dihydroxy-4pregnen-3-one (17α,20β-DHP). Data are presented as the mean \pm mean standard error (mean \pm MSE). $n = 3$ per experimental group. Values followed by letters are significantly different the dominant, nondominant females, and control group ($p < 0.05$).

3.4. Histological and Immunohistochemical Analyses of the Ovarian, Brain, and Pituitary Glands

Histological analyses of the ovaries identified the following phases of oocyte development in females of all groups: vitellogenic oocytes (Figure 4a) with nuclear migration (Figure 4b,c) and postovulatory follicles (Figure 4d), in addition to several reserve oocytes

(perinucleolar oocytes) (Figure 4). There were no qualitative differences between experimental groups in the histological analyses.

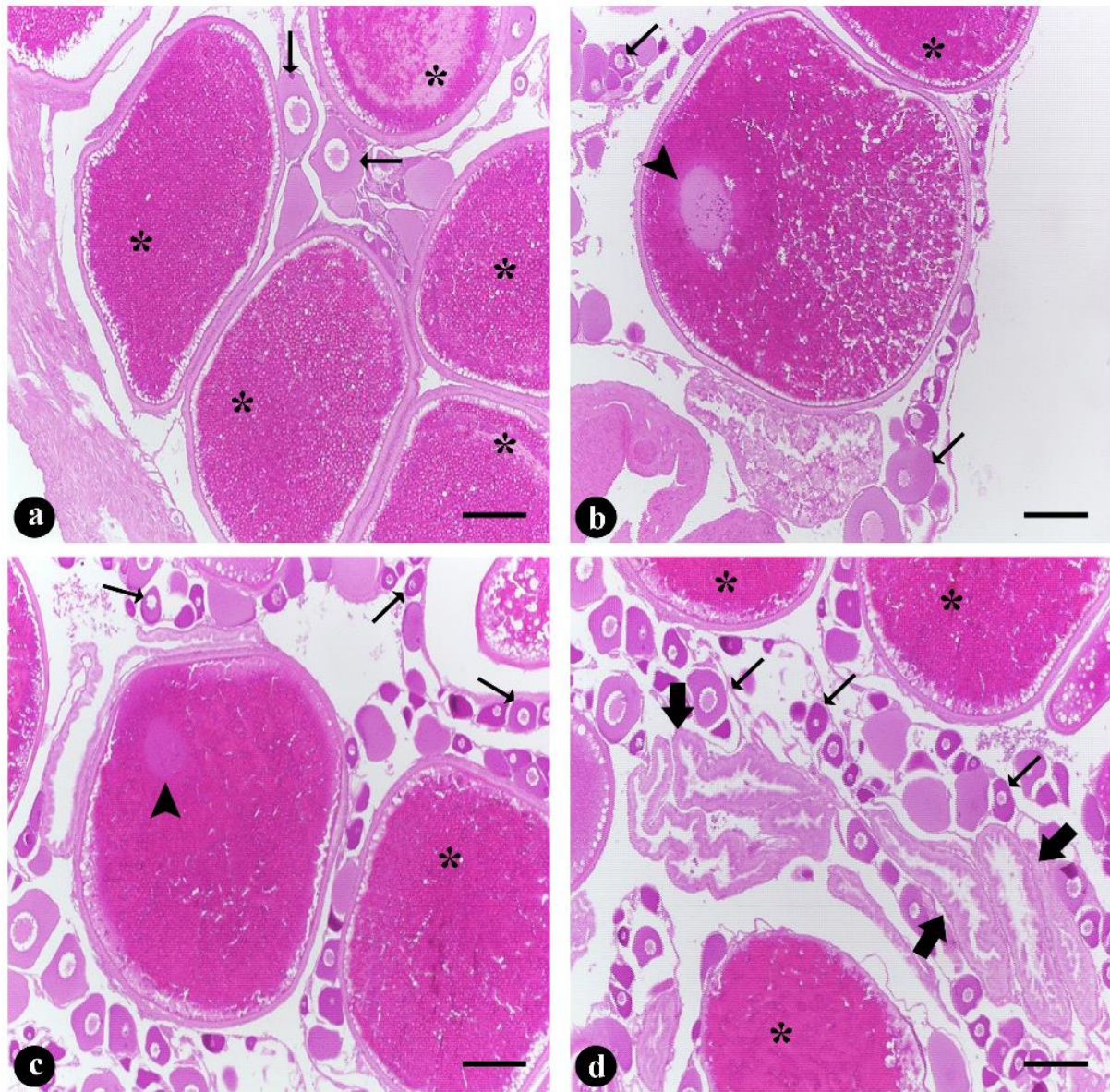


Figure 4. (a–d) Micrographs of the ovaries of *Steindachmeridion parahybae* in captivity showing different germ cell types observed in the control, dominant and nondominant females. (a) Vitellogenic oocytes (asterisk); (b,c) vitellogenic oocytes with nuclear migration (arrowhead) and vitellogenic oocytes (asterisk); and (d) vitellogenic oocytes (asterisk) and postovulatory follicle (thick arrow). Thin arrows (all images) indicate reserve oocytes, namely, perinucleolar oocytes. Haematoxylin and eosin stain. Scale bars: 300 µm.

Figure 2c–e shows a schematic sagittal section of an adult brain of *S. parahybae*. The lines indicate levels of transverse histological sections of the main nuclei resulting from the identification of AVT neurons. The preoptic area (POA) (Figure 2c–e) in *S. parahybae* extends from the ventral telencephalon region (Tel) to the beginning of the diencephalon. It surrounds the anterior diencephalic ventricle portion, also known as the third ventricle. Moreover, the main nuclei of POA were identified based on cell size distribution: parvocellular, magnocellular, and gigantocellular, respectively (Figure 5a,c,e).

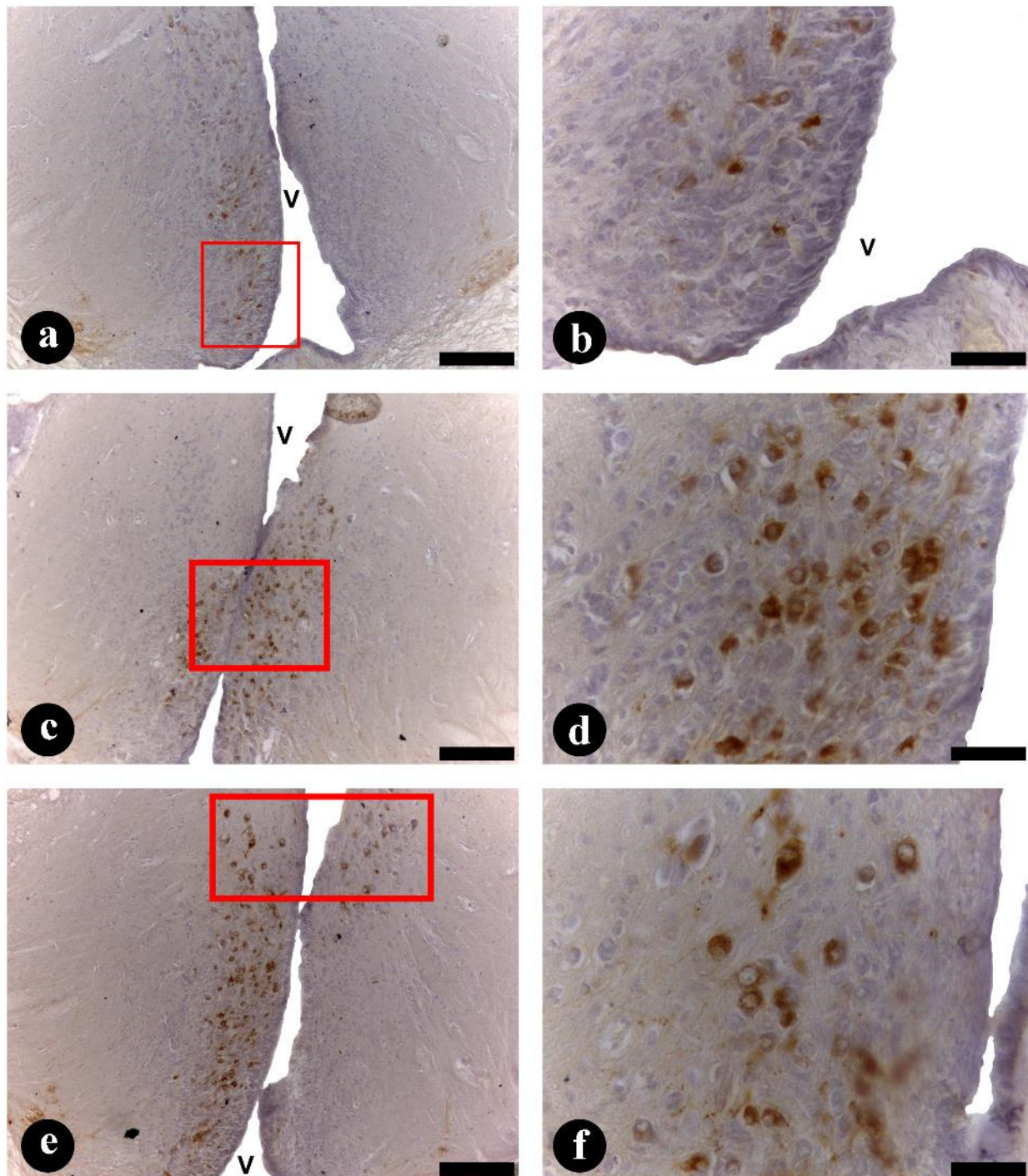


Figure 5. (a–f) Transversal sections through the preoptic area (POA) of *Steindachneridion parahybae* brain. (a,b) Arginine-vasotocin (AVT) immunoreactive (ir) neurons in the parvocellular (pPOA) subpopulations (a) and details of AVT-ir (b); (c,d) arginine-vasotocin immunoreactive neurons in the magnocellular (mPOA) subpopulations (c) and details of AVT-ir (d); (e,f) arginine-vasotocin immunoreactive neurons in the gigantocellular (gPOA) subpopulations (e) and details of AVT-ir (f). Scale bars: 100 μm (a,c,e); 10 μm (b,d,f).

Adult *S. parahybae* females showed AVT-ir neurons exclusively inside the POA area (pPOA, mPOA, and gPOA subpopulations) (Figure 5). AVT-ir cell bodies located in the pPOA area (Figure 5a,b) were the most rostral, ventral, and numerous cells, round or oval in shape, and presented smaller cellular and eccentric nuclear areas (102.37 ± 3.40 and $72.40 \pm 1.19 \mu\text{m}^2$,

respectively) than other cell subpopulations. The mPOA neurons (Figure 5c,d) extended more dorsally and posteriorly from the pPOA. They were numerous and round or pyriform in shape, with a larger cellular and eccentric nuclear area (157.93 ± 2.76 and $78.55 \pm 1.28 \mu\text{m}^2$, respectively) than pPOA cells. Finally, in more dorsal and posterior positions were the gPOA cell subpopulation (Figure 5e,f). These cells are characterized by an irregular shape, the largest cellular area ($245.43 \pm 4.10 \mu\text{m}^2$) inside the POA area, and presented more spherical and eccentric nuclei ($146.14 \pm 2.74 \mu\text{m}^2$) than pPOA and mPOA cells. AVT-ir cell bodies were located in the pPOA, mPOA, and gPOA subpopulation borders of the third ventricle (Figure 5). Table 3 shows the cellular and nuclear area of each subpopulation.

Table 3. Morphometric analysis (cellular and nuclear area— μm^2) of arginine-vasotocin immunoreaction neuron of *Steindachneridion paraguayae* female in the different preoptic area of the brain: parvocellular (pPOA); magnocellular (mPOA), and gigantocellular (gPOA) areas. $n = 3$ animals; $n = 10$ cellular and nuclear area per animal measured; totalizing 30 cells/nucleus per experimental group. Data are presented as the mean \pm mean standard error (mean \pm MSE).

Cellular Subpopulations in the Preoptic Area	Cellular Area (μm^2)	Nuclear Area (μm^2)
Parvocellular (pPOA)	102.37 ± 3.40^a	72.40 ± 1.19^a
Magnocellular (mPOA)	157.93 ± 2.76^b	78.55 ± 1.28^b
Gigantocellular (gPOA)	245.43 ± 4.10^c	146.14 ± 2.74^c

Values followed by different letters (a,b,c) are significantly different between brain areas ($p < 0.05$).

The most dense AVT-ir axonal projections occurred inside the POA area, mainly in the ventral area of POA (Figure 6a,b). These AVT-ir fibers processes appeared to project both towards the Pi gland, as seen in Figure 6c,d. At the Pi gland (anterior pituitary, adenohypophysis), there were AVT-ir fibers at the proximal pars distalis and at the pars intermedia, while at the rostral pars distalis (Figure 6c,d), no positive IHC reaction was observed.

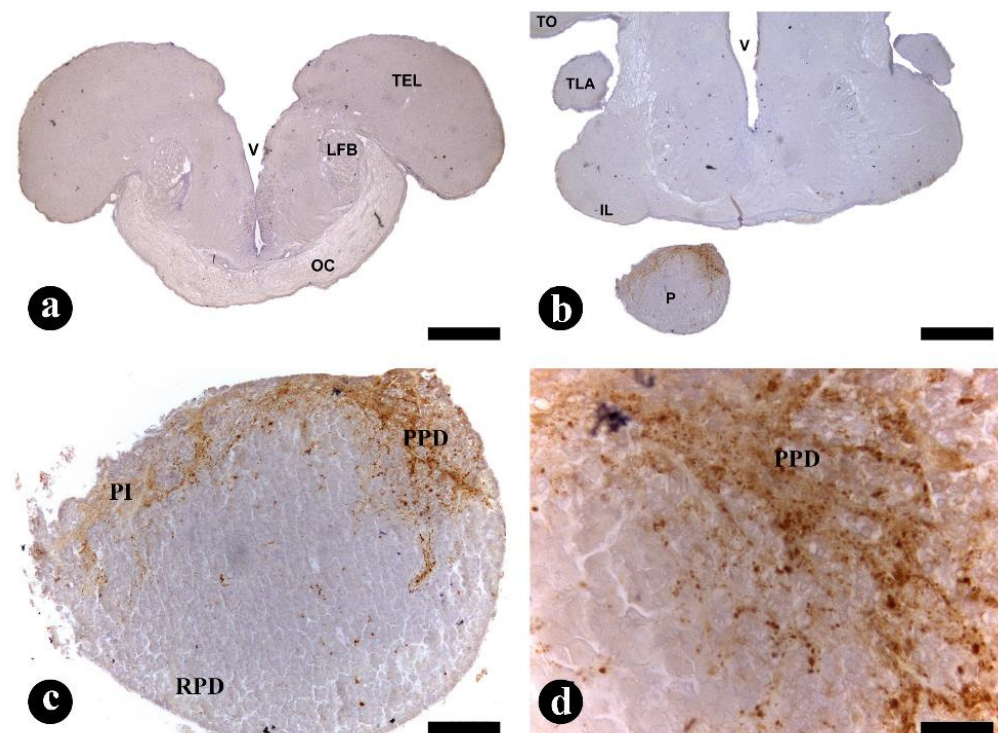


Figure 6. (a–d) Transversal sections through the preoptic area (POA) and pituitary (Pi) gland of *Steindachneridion paraguayae*. Distribution of fibers immunoreactive (ir) with arginine-vasotocin (AVT)

antisera (a–d). Details of strong and several fibers-ir lengthways with AVT antisera in the ventral POA area and Pi gland. At the Pi gland, mainly in proximal pars distalis (PPD) and pars intermedia (PI), while in rostral pars distalis (RPD). IL, inferior lobe; LFB, lateral forebrain bundle; OC, optic chiasma; P, pituitary gland; TEL, telencephalon; TLA, nucleus of the lateral torus; TO, tectum optic; V, ventricle; Scale bar: 100 μm (a,b); 50 μm (c); 10 μm (d).

3.5. Morphometry of AVT-ir Cellular and Nuclear Areas in POA Area and between Dominant vs. Nondominant Females

The cellular and nuclear area of AVT-ir neurons of the *S. parahybae* brain differ among subpopulations (pPOA, mPOA, and gPOA) (Table 3). The gPOA cells showed larger cellular and nuclear areas than mPOA cells ($p < 0.01$ for both areas) and pPOA ($p < 0.02$ for cellular area and $p < 0.01$ for nuclear area). In turn, pPOA cells showed smaller cellular and nuclear areas than mPOA cells ($p < 0.01$ for both areas).

The comparison of the cellular and nuclear area between experimental groups revealed variations in nuclear area among the mPOA subpopulation. There were smaller areas in the ND group in relation to the control and D groups ($p < 0.006$). There were no differences between pPOA and gPOA subpopulations (Table 4). Regarding GnRH, there were differences in the cellular area for cfGnRH, with lower values in the ND group in relation to the control and D groups ($p < 0.05$) (Table 4). Regarding cGnRH-II, there were differences in nuclear area, showing lower values in the ND group in relation to the control and D groups ($p < 0.05$) (Table 4). Regarding luteinizing hormone (b-LH), both areas (nuclear and cellular) were smaller in the ND group than in the control and D groups ($p < 0.05$) (Table 4).

Table 4. Morphometric analysis (cellular and nuclear area— μm^2) of arginine-vasotocin in distinct region (AVT pPOA = parvocellular, AVT mPOA = magnocellular, and AVT gPOA = gigantocellular), catfish gonadotropin-releasing hormone (cfGnRH) and chicken-II gonadotropin-releasing hormone (cGnRH-II) immunoreaction neuron and β -luteinizing hormone (β -LH) immunoreaction cells in control, dominant and nondominant of *Steindachneridion parahybae* female. For AVT: $n = 3$ animals; $n = 10$ cellular and nuclear area per animal measured; totalizing 30 cells per experimental group; for cfGnRH and cGnRH-II: $n = 3$ animals; $n = 8$ cellular and nuclear area per animal measured; totalizing 24 cells per experimental group; for β -LH: $n = 3$ animals; $n = 15$ cellular and nuclear area per animal measured; totalizing 45 cells per experimental group. Data are presented as the mean \pm mean standard error (mean \pm MSE).

Cellular Subpopulations in the Preoptic Area	Control		Dominant		Nondominant	
	Cellular Area	Nuclear Area	Cellular Area	Nuclear Area	Cellular Area	Nuclear Area
AVT pPOA	103.11 \pm 3.20 ^a	74.10 \pm 2.50 ^a	102.18 \pm 2.10 ^a	72.44 \pm 2.10 ^a	102.56 \pm 3.60 ^a	72.36 \pm 1.24 ^a
AVT mPOA	157.77 \pm 3.24 ^a	77.20 \pm 1.85 ^a	159.76 \pm 4.34 ^a	75.25 \pm 1.17 ^a	156.10 \pm 1.77 ^a	61.86 \pm 1.77 ^b
AVT gPOA	254.52 \pm 7.34 ^a	137.50 \pm 4.22 ^a	243.61 \pm 7.42 ^a	146.60 \pm 4.39 ^a	247.24 \pm 3.92 ^a	145.68 \pm 3.54 ^a
cfGnRH	27.34 \pm 0.99 ^a	13.07 \pm 0.44 ^a	26.31 \pm 1.49 ^a	12.97 \pm 0.63 ^a	23.78 \pm 0.71 ^b	11.01 \pm 0.45 ^a
cGnRH-II	28.31 \pm 1.33 ^a	11.59 \pm 0.55 ^a	26.45 \pm 1.27 ^a	10.61 \pm 0.54 ^a	25.09 \pm 1.27 ^a	7.89 \pm 0.27 ^b
β -LH	14.40 \pm 0.44 ^a	6.80 \pm 0.96 ^a	13.46 \pm 0.22 ^a	6.93 \pm 0.24 ^a	12.11 \pm 0.43 ^b	6.54 \pm 0.11 ^b

Values followed by different letters (a,b) are significantly different between brain areas ($p < 0.05$).

Figure 7 summarizes the results obtained via semi-quantitative analysis. In general, ND females showed lower OD values in relation to control and D females. Regarding AVT, OD values were lower in pPOA, and mPOA and gPOA in ND (176.33 ± 11.29 , 193.67 ± 6.25 , and 189.00 ± 5.52 a.u., respectively), than the control (262.50 ± 2.92 , 259.75 ± 1.89 , and 263.25 ± 1.75 a.u., respectively) ($p \leq 0.001$) and D (242.33 ± 15.27 , 237.67 ± 5.42 , and 248.33 ± 5.88 a.u., respectively) ($p \leq 0.001$). Only mPOA OD values differed control females from D females ($p \leq 0.001$). Regarding GnRH OD values, cfGnRH and cGnRH-II were low in the ND group (105.00 ± 1.95 and 140.15 ± 6.57 a.u., respectively) compared to the control (134.51 ± 3.88 and 194.16 ± 6.23 a.u., respectively) ($p \leq 0.001$) and the D group (130.72 ± 5.50

and 200.40 ± 8.87 a.u., respectively) ($p \leq 0.001$). Regarding β -LH, the same pattern of difference occurred, with lower OD values in the ND group (118.12 ± 1.30 a.u.) compared to control females (143.65 ± 1.88 a.u.) and D females (142.13 ± 1.81 a.u.) ($p \leq 0.001$).

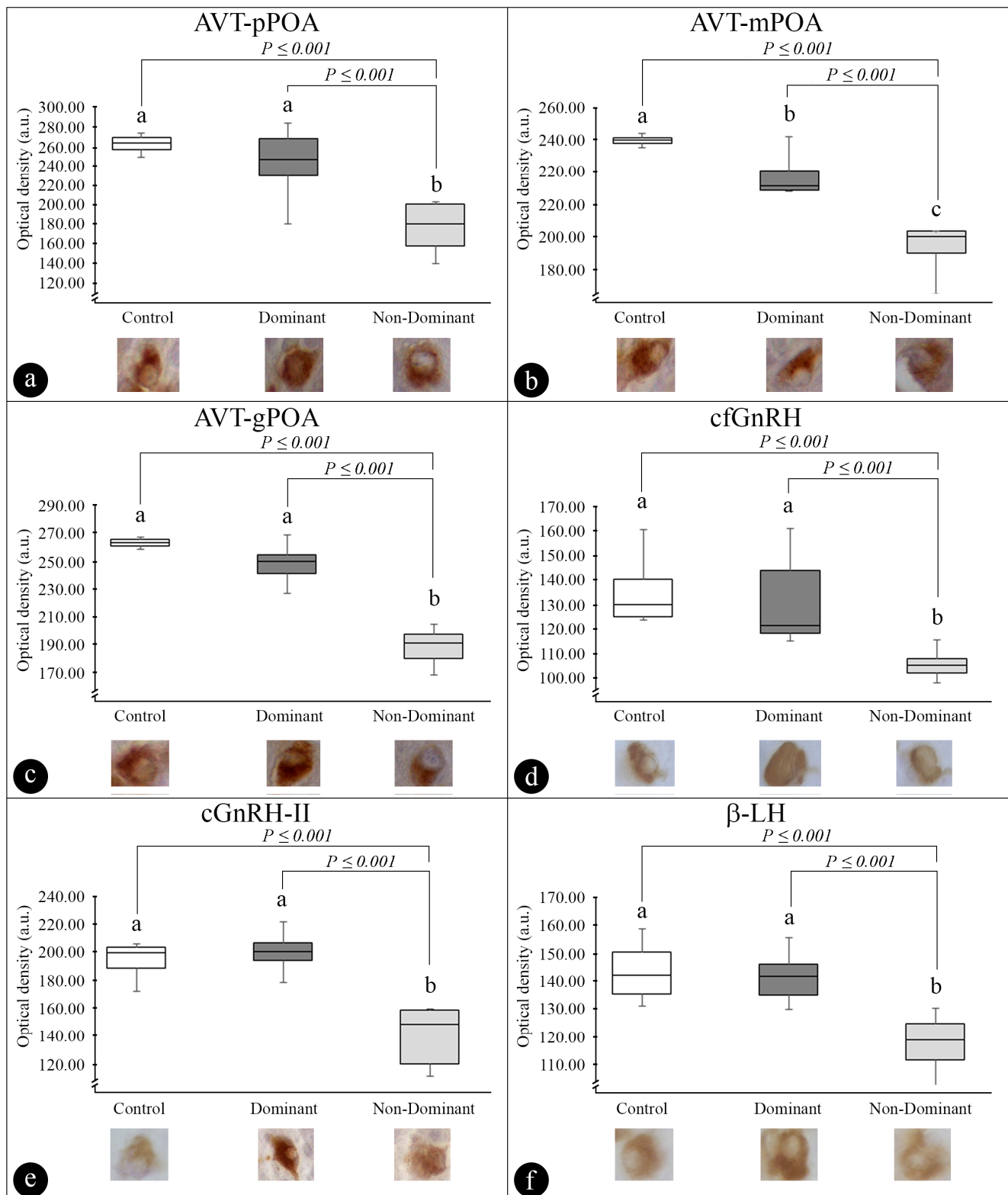


Figure 7. (a–f) Semiquantitative analysis (optical density (OD), a.u.) of immunohistochemistry of the arginine-vasotocin (AVT) and gonadotropin-releasing hormone (GnRH) neuronal system and

gonadotropins (LH) of *Steindachneridion paraguayae* in the different experimental groups, control, dominant, and nondominant females. (a) AVT-pPOA: parvocellular arginine-vasotocin subpopulation; (b) AVT-mPOA: magnocellular arginine-vasotocin subpopulation; (c) AVT-gPOA: gigantocellular arginine-vasotocin subpopulation; (d) cfGnRH: catfish gonadotropin-releasing hormone; (e) cGnRH-II: chicken-II gonadotropin-releasing hormone; (f) β -LH: β -luteinizing hormone. For AVT: $n = 3$ animals; $n = 10$ for OD of immunostaining per animal measured; totalizing 30 cells per experimental group; for cfGnRH and cGnRH-II: $n = 3$ animals; $n = 8$ for OD of immunostaining per animal measured; totalizing 24 cells per experimental group; for β -LH: $n = 3$ animals; $n = 15$ for OD of immunostaining per animal measured; totalizing 45 cells per experimental group. Values followed by different letters (a,b,c) represent significantly different ($p < 0.05$).

The main Pearson's correlation results are presented in Figure 8. Plasma Cort had a positive correlation in control and D animals with 17α -20 β -DHP and β -LH, but a negative correlation in ND animals. As for androgens, a positive correlation was identified between Cort and 11-KT for all groups, as well as for T for D and ND (positive) and negative for the control (Cort and T). Furthermore, plasma Cort also showed a positive correlation for the different AVT subpopulations in the D animals and the control group, but a negative correlation only for the mPOA subpopulation in the ND animals. As the animals in the present study were artificially induced to reproduce, there was a positive correlation between β -LH and 17α -20 β -DHP (all groups). On the other hand, 17α -20 β -DHP showed a positive correlation with AVT pPOA and AVT gPOA and a negative correlation with AVT mPOA (both for D and control animals) and a positive correlation with mPOA was identified in ND females. Inversely to what was identified in ND animals, as 17α -20 β -DHP was positive for AVT mPOA and negative for AVT pPOA and AVT gPOA. Positive correlation between AVT (mPOA, gPOA and pPOA) with cfGnRH, cGnRH-II and β -LH were observed in practically all groups, except for mPOA with β -LH (negative) and between pPOA and cGnRH-II (no interaction) in the group D females.

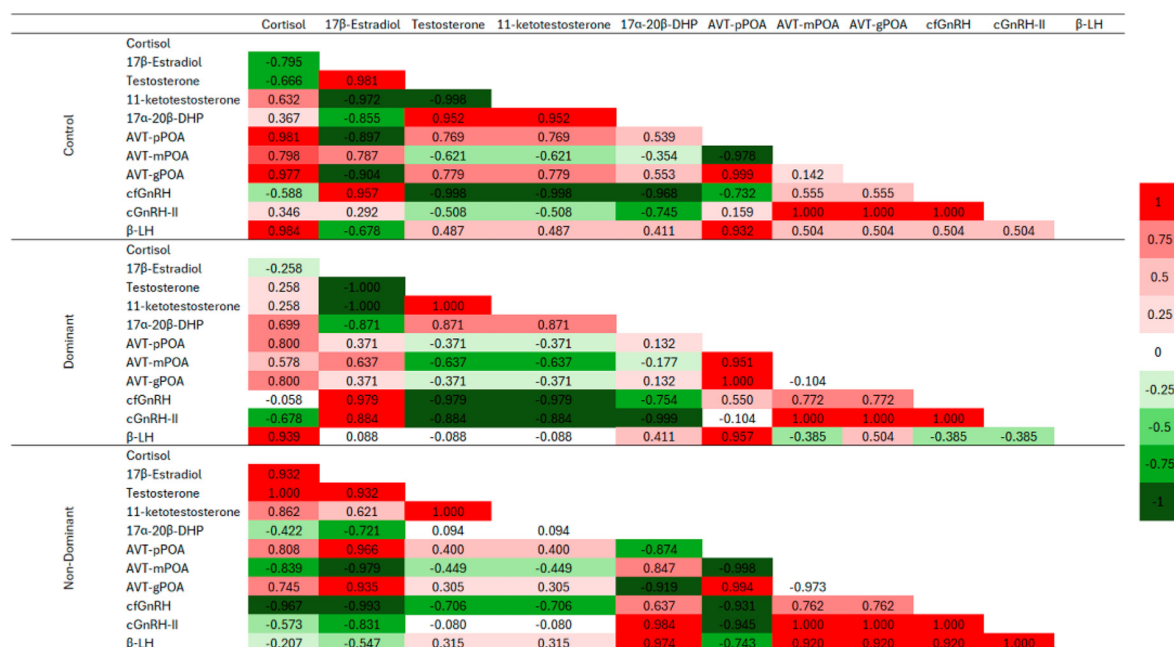


Figure 8. Pearson's correlation coefficient matrix showing potential relationships between sexual steroids, cortisol plasma concentration and optical density (a.u.) of immunohistochemistry of the arginine-vasotocin (AVT), gonadotropin-releasing hormone (GnRH) neuronal system and gonadotropins (LH) of *Steindachneridion paraguayae* in the different experimental groups, control, dominant, and nondominant females. The color of each box indicates the relationship between

the various parameters examined in this study, with dark red indicating positive relationships and dark green indicating negative relationships. Abbreviations: AVT-pPOA: parvocellular arginine-vasotocin subpopulation; AVT-mPOA: magnocellular arginine-vasotocin subpopulation; AVT-gPOA: gigantocellular arginine-vasotocin subpopulation; cfGnRH: catfish gonadotropin-releasing hormone; cGnRH-II: chicken-II gonadotropin-releasing hormone; β -LH: β -luteinizing hormone; and 17α -20 β -DHP: 17α -20 β -dihydroxy-4-pregnen-3-one.

4. Discussion

4.1. Water Parameters and General Characteristics of the Breeders

The water quality parameter values of the present study were within the comfort zone of this species, and close to previous research performed for maintaining and rearing of broodstocks of wild *S. parahybae* [3] and captivity females [4,5]. The reproductive data of *S. parahybae* in captivity (i.e., hormonal induction response, quantity of oocytes released, fertilization rate) have been extensively discussed in previous studies [3–5,7,11] and the results obtained in the present study did not differ from the reproductive pattern observed for *S. parahybae* in captivity. Regarding the histological analyses of the ovaries, the phases of oocyte development during the reproductive cycle of *S. parahybae* in captivity were also widely discussed [11]. The present study also corroborated that *S. parahybae* females can experience multiple spawning events during the reproductive cycle, because, after artificial induction, postovulatory follicles and several vitellogenic oocytes with nuclear migration and vitellogenic oocytes were identified in these animals that had been induced and spawned. More information on induced reproduction of *S. parahybae* can be found in [3–5,7,11].

4.2. Vasotocinergic System Characterization, and Social Status: Dominant and Nondominant Females

This study initially characterized the vasotocinergic system and its potential association with reproductive physiology and social behavior of *S. parahybae* females. In this species, AVT-ir neurons are located exclusively inside the POA and distributed among parvo, magno, and gigantocellular subpopulations. The pPOA subpopulation is located at the rostral and ventral region of the POA. It is potentially important in mediating stress responses in fish. The mPOA and gPOA subpopulations are located more caudally and dorsally to pPOA; it distinguishes pPOA neuron by morphology, soma size, and most caudal distribution. Studies have linked both cellular subpopulations (mPOA and gPOA) to behavioral functions, such as territorial behavior, but there are variations in distribution that suggest specificity. This pattern of distribution is consistent with all vertebrate species studied to date, including agnathans and gnathostomes. These cells project to a variety of brain regions and to the pituitary gland [20,28] in teleost species such as butterflyfish (*Chaetodon miliaris* and *C. multicinctus*) [48], medaka (*O. latipes*) [49], goldfish (*Carassius auratus*) [50], and pupfish (*Cyprinodon nevadensis*) [51]. AVT-ir neurons are located almost exclusively in the POA and the anterior hypothalamus, distributed among a population of densely packed small cells and two other populations of larger cells surrounding the recess of the third ventricle, the pPOA, mPOA, and gPOA. Analyzing butterflyfish (*C. multicinctus* and *C. miliaris*), Dewan et al. [48] described a group of additional AVT-ir neurons in the ventral tubular hypothalamus with even smaller soma diameter than pPOA cells. This population did not appear in *S. parahybae* and *chanchita* (*C. dimerus*) [30]. Direct evidence from the observation of axonal projections into the pituitary gland of *S. parahybae* suggest a possible role of AVT at a central level acting as a neuromodulator or as a neurohormone with target sites such as the pituitary, mainly to proximal pars distalis (PPD) (next to gonadotropins, mainly β -LH) [9], and is discussed below.

In general, the morphometric analysis (cellular and nuclear area) of AVT-ir in D and ND of *S. parahybae* did not reveal differences. However, the gene expression analysis in peacock blenny (*Salaria pavo*) [35,36], toadfish (*Porichthys notatus*) [52], and Azorean rock-pool blenny (*Parablennius parvicornis*) [53] indicated low AVT gene expression levels

and/or soma size in these subpopulations (pPOA, mPOA, and gPOA) when associated with territorial behavior. Other species, such as zebrafish (*D. rerio*) [54], African cichlid fish (*Astatotilapia burtoni*) [19], anemonefish (*Amphiprion ocellaris*) [55], and *chanchita* (*C. dimerus*) [30], presented an opposite pattern, that is, high AVT levels associated to territoriality. In this case, several previous findings have shown that AVT differentially expresses in these subpopulations (pPOA, mPOA, and gPOA), which directly affect the behavior of many fish species [24]. These studies have indicated differences in AVT gene expression, suggesting differences in descriptions of anatomy [19,54].

In relation to behavior, females that were kept in the same tank presented lesions on the skin caused by aggressive behavior. As only one female presented injuries, one was considered D and the other ND (subordinate). Caneppele et al. [3] have reported this aggressive behavior after hormonal induction to start the reproduction of *S. parahybae*. In that experiment, a broodstock couple was kept in the same tank (females were more aggressive than males; males did not show aggressive behavior at any time during the reproductive process). Honji et al. [4] reported that when two females were kept in the same tank, the results were the same (very aggressive females). Therefore, keeping two animals (a couple or females) during hormonal induction of this species is not recommended. Moreover, among social animals, dominance can have long-term physiological consequences. There are strong interactions between behavior and the endocrine and nervous systems that affect the interactions between an animal and its environment, including social interactions [30,56]. Although social regulation is a well-established phenomenon on several physiological processes, little is known about the mechanisms linking an aggressive behavior to reproductive physiological changes associated with dominance. Furthermore, the relationship between aggressive behavior and reproductive dysfunction in rheophilic species, when kept in captivity, is not known. Therefore, the present study is a starting point in this context with *S. parahybae*.

4.3. AVT System Influences the Brain-Pituitary-Gonads Axis of *Steindachneridion parahybae*

Similar to the conserved pattern observed here for positive AVT immunoreaction, vasotocinergic fibers also show a high degree of neuroanatomical conservation. Vasotocin projections appear throughout teleost brains, especially the forebrain and hindbrain regions [22]. As with the few species examined thus far, there is considerable anatomical overlap between GnRH and AVT neurons. In *chanchita* *C. dimerus*, the greatest density of AVT-ir axons is observed within the POA, where fibers form a dense preoptic-hypophyseal tract entering the pituitary through the anterior and posterior infundibular stalks. This preoptic-hypophyseal area is one of the primary regions where GnRH neurons are located in this species [30]. In the electric fish species *Gymnotus omarorum* and *Brachyhypopomus gauderio*, AVT-ir fibers run ventro-caudally to the pituitary and the lateral and ventral hypothalamus [22], likely indicating the location of GnRH neurons. There is a colocalization of AVT receptor with GnRH in hypothalamic neurons of rock hind (*Epinephelus adscensionis*) and *corvina blanca* (*Micropogonias albus*) [57]. In *S. parahybae*, an anatomical overlap between GnRH [10] and AVT (present study) was also identified.

Neurophysiological studies in the rainbow trout (*Oncorhynchus mykiss*) show that both sGnRH (salmon GnRH) and cGnRH-II facilitate the electrical activity of POA AVT neurons [58]. This indicates that both hypothalamic and midbrain GnRH may modulate AVT neurons regulating reproductive behaviors. Increases in the number or size of GnRH neurons are known to reflect differences in the potential to deliver GnRH to the pituitary and stimulate steroidogenesis. Consequently, data on body size influences on GnRH (and AVT) cell size and number are noted where available [34]. In teleosts, numerous investigations have highlighted the significance of AVT neurons in shaping agonistic phenotypic asymmetries. Changes in both the quantity and size of AVT neurons have been detected through techniques such as immunohistochemistry and in situ hybridization. Despite the differences in experimental approaches among these studies, it is clear that the consolidation of dominance is associated with enduring morphological changes in AVT neurons,

and that these changes do not affect all the subpopulations of AVT cells in a homogeneous way [22]. For *S. parahybae*, due to the few differences in the cellular and nuclear area of the distinct AVT subpopulations that were observed between the experimental groups, we preferred to use the OD-ir in comparisons. A positive correlation between mPOA, gPOA, and pPOA with GnRH (cfGnRH and cGnRH-II) and β -LH were observed in practically all groups. These results aligned with the existing literature, demonstrating that the combination of GnRH and AVT during artificial induction, especially with the second dose injection, does not significantly impact the efficiency of spawning, egg production, fertilization rate, hatching rate, or survival rate postspawning [57]. Although the present study did not inject AVT, a positive correlation between GnRH, β -LH, and progestins with AVT can suggest that AVT is a powerful indicator in the induction of *S. parahybae* as well. Therefore, exploring the differences in the actions of AVT and GnRH in the POA is crucial for understanding the neuroendocrine basis of reproductive plasticity among teleosts [34]. Further studies are needed to determine the short- and long-term effects of GnRH release on AVT neurons (and vice versa) and the physiological processes and behaviors regulated by these neuropeptides in *S. parahybae* and other Neotropical species.

In *S. parahybae* there is a greater association between positive AVT of POA area immunoreactive to the pituitary gland, suggesting a possible role of AVT as a moderating factor for the release of pituitary hormones, mainly in D and control animals and in the pPOA and gPOA AVT subpopulations with β -LH observed as a positive correlation. Moderate negative correlation in ND animals between pPOA and β -LH was identified. Ramallo et al. [30] describe that the AVT affects the release of both gonadotropins in *chanchita* (*C. dimerus*). In rock hind (*E. adscensionis*), Maruska et al. [58] described the presence of AVT receptors in the proximal pars distalis (PPD) in the adenohypophysis but not in the neurohypophysis, also suggesting that AVT is a neurotransmitter or neuromodulator of gonadotropins. Additionally, the effects of AVT have been noted on gonadotropin release in Sailfin molly (*Poecilia latipinna*) as described by Maruska et al. [58]. It is noteworthy that the above-mentioned studies, which report AVT fibers broadly across the brain of different fish species, have used frozen immunohistochemistry protocols, different from the paraffin-based protocol used here. It is possible that the failure of detecting fibers outside the POA area and hypothalamic region results from methodological issues. This type of discussion was also a topic with *chanchita* (*C. dimerus*) [30], and the present study corroborated this methodological information. Additionally, it is possible that the pPOA nucleus, which projects into the pituitary gland [20,28,59], may be involved in the modulation of behaviors related to submission and/or activation of the stress axis [28,60]. This was not possible to report in the present study. Evidence from other teleost species shows that AVT synthesized by pPOA cells is involved in regulating the release of Cort through the action of AVT on the HPI axis (hypothalamus-pituitary-interrenal) [20,28]. Fox et al. [60], Ramallo et al. [30], and Martos-Sitcha et al. [28] reported that the level of the stress hormone Cort depends critically on social and reproductive status of an individual and on the stability of its social situation. The findings here showed that Cort varied between females and may be responsible for the low reproductive performance of ND *S. parahybae* in captivity. This is in agreement with the notion that subordination is associated with high stress levels, marked by high plasma glucocorticoids. Increased cortisol secretion is a primary indicator of stress in teleost fish [61,62], as observed in *chanchita* (*C. dimerus*) [56,63,64] and African cichlid fish (*A. burtoni*) [60,65,66], and in many other vertebrates' species [67]. This scenario cannot be confirmed for *S. parahybae* but suggests a behavior and possibly an AVT affecting the HPI axis of this species (due to the increase in Cort in ND females).

Larson et al. [54] only observed AVT immunostaining in the pPOA of zebrafish (*D. rerio*) subordinates. It was absent in dominant males. Likewise, in *chanchita* (*C. dimerus*) AVT showed a positive and concentration-dependent effect over testicular androgens synthesis and secretion in vitro [30]. The authors also reported AVT gene expression in testicular somatic tissue located in the interstitial compartment. Thus, the AVT system in *chanchita* (*C. dimerus*) males seems to be of high complexity, with multiple sites of action. Despite

differences in methodological and behavioral paradigms, these studies, corroborating this study's data on *S. parahybae*, point to a putative role of the AVT neuronal system in activating/modulating submissive neural circuits or inhibiting aggressive/dominance neural networks, as well as high Cort levels, through the action of AVT on the HPI axis. At a central level, it could act jointly by inducing typical aggressive behaviors. Even though the effect of AVT on the stress axis is well characterized for some species, information on this context is lacking for Neotropical teleost species (AVT neuronal system and influence of BPG and/or HPI axis).

High E₂ plasma levels precede secondary growth (or vitellogenic oocytes). This is related to the synthesis of vitellogenin because one of the main actions of estrogen is to stimulate the synthesis of vitellogenin in the liver, then incorporating it into the oocyte. E₂ plasma concentrations are high during primary growth in several species, occurring before the presence of vitellogenic oocytes and ovulation [15, for review], including were observed in *S. parahybae* [11]. The results obtained in the present study using histological analysis revealed that females are sexually mature females (with vitellogenic oocytes). However, there were no differences in the plasma E₂ concentrations between experimental groups.

Although T is considered in the synthesis of E₂ and 11-KT [68,69], several studies have detected the presence of high androgen concentration during the reproduction cycle of females [70,71]. However, in the present study, there were no differences in plasma T profile between experimental groups. In the present study, the 11-KT concentration was higher in all groups, and females showed vitellogenic oocytes. This scenario suggests an important physiological role during the gonadal maturation of *S. parahybae*. However, the 11-KT plasma concentration between ND and D females was not statistically different. The literature reports that the variation of this steroid is related to the social hierarchy presented by cichlids [63,64,72,73], suggesting that the participation of androgens may be species-specific.

Unfortunately, the maintenance of *S. parahybae* broodstock in captivity was not completely successful [3,4,9–11]. This was due to endocrine disruption in the synthesis and/or release of LH [9] and GnRH [10], as well as the sexual steroid pathway [11]. 17 α -20 β -DHP is the most effective progestogen for inducing the breakdown of the germinal vesicle (GVBD) in most teleost species examined to date [74]. The concentration of plasma 17 α -20 β -DHP is low in teleost fish blocked from migrating (reophilic species) or when kept in captivity in fish rearing operation (aquaculture of reophilic species for example). This situation negatively affects final oocyte maturation in teleost species. Observations of the hormones produced by the BPG axis are important for understanding the possible physiological causes of reproduction failures [14–18,74]. In the present study, control and D females presented a plasma profile of this sexual steroid superior to ND females, which culminated in a better reproductive performance.

Finally, there are well-known trade-offs between glucocorticoids and sexual steroid hormones in fish physiology, mainly in the context of social (stress) and aggressive behavior, as reported by Silva and Pandolfi [22], Balment et al. [26], and Ramallo et al. [30], including the participation of AVT and AVT-crosstalk with other reproductive neurohormones, such as GnRH, with pituitary hormones, as β -LH, and gonadal steroid hormones, such as E₂, T, and 11-KT [16,18,20,22,24,26,30,69,75], a profile that was also corroborated in the present study with *S. parahybae*. In the literature, the vast majority of studies on the influence of AVT with gonadal steroids were carried out with male fish, in which AVT has direct effects on the release/production of testicular androgens, as carried out in *C. dimerus* [30]. In *S. parahybae* female, although AVT presents a positive correlation with androgens (T and 11-KT), it was only identified in the pPOA and gPOA subpopulations in control and ND group. The mPOA subpopulation showed a negative correlation in all experimental groups and may suggest a specific action depending on the AVT subpopulation. Interestingly, mPOA presented a negative correlation with 17 α -20 β -DHP in the control and in D females (contrary to the ND females, as it was a positive correlation), suggesting an inverse interaction between mPOA and 17 α -20 β -DHP, suggesting that this steroid can be one of the

strong candidates for FOM in teleost fish species [74]. Therefore, the present study also fills this gap in the reproductive physiology of endangered Neotropical fish, mainly in species where females are more aggressive and present reproductive dysfunctions when reared in captivity.

5. Conclusions

The results obtained here suggest a possible direct effect of aggressive behavior on the AVT or the GnRH neuronal system and an indirect effect (through pituitary hormone) on steroidogenesis in *S. parahybae*. Thus, AVT may not only be associated with aggressive behaviors at a central level, acting as neuromodulator, but it may also act as a neurohormone and putative pituitary hormone-releasing factor, modulating the sex steroid pathway in the gonads. Control and D females showed a higher level of 17α - 20β -DHP and a lower level of Cort than ND females. Therefore, in *S. parahybae*, the AVT neuronal system is highly complex, possibly presenting multiple sites of action along the BPG axis. AVT neuronal systems are directly and/or indirectly associated with behavioral and physiological changes that are typical to *S. parahybae* females when induced artificially to spawning in captivity. Finally, the results contribute to an improved reproductive performance in captivity since the endangered status of the species deserves special attention and urgent actions, especially improving the understanding of their reproductive physiology, which is the basic premise for fish restocking program in the Paraíba do Sul River basin.

Author Contributions: R.M.H.: Conceptualization, Funding acquisition, Data curation, Formal analysis, Investigation, Methodology, Visualization, Writing—original draft, Writing review & editing. B.C.A.; M.R.R.; L.M., P.H.d.M. and D.C.: Investigation, Methodology, Formal analysis, Writing review & editing. R.G.M.: Conceptualization, Data curation, Funding acquisition, Investigation, Methodology, Supervision, Writing review & editing. All authors have read and agreed to the published version of the manuscript.

Funding: This work was supported by the FAPESP (*Fundação de Amparo à Pesquisa do Estado de São Paulo*: FAPESP: 2007/55494-7, 2008/57687-0, 2017/06765-0); the *Programa de Mobilidade Internacional de Alunos de Pós-Graduação—Santander/Banespa*; and CAPES (*Coordenação de Aperfeiçoamento de Pessoal de Nível Superior*): finance code (001). RGM is a recipient of the CNPq (*Conselho Nacional de Desenvolvimento Científico e Tecnológico*) productivity scholarship.

Institutional Review Board Statement: All procedures were based on the guidelines of the Brazilian Federal Law (number 11.794, of 8th October 2008), which established the procedures for the scientific use of animals, and São Paulo State Law (number 11.977, of 25 August 2005), which established the Animal Protection Code of the São Paulo State and other rules applicable to the use of animals for teaching and scientific purposes. Field collections were authorized by the ICMBio (*Instituto Chico Mendes de Conservação da Biodiversidade*: authorization number: 34938-1) and fish euthanasia were approved by the CEUA/IB/USP (*Comissão de Ética no Uso de Animais, Instituto de Biociências, Universidade de São Paulo*: protocol number: 072/2008).

Informed Consent Statement: Not applicable.

Data Availability Statement: All data generated or analyzed during this study are included within this article.

Acknowledgments: We are especially grateful to: (1) Matthew Grober (Georgia State University, Atlanta, USA) for the kind donation of arginine-vasotocin antibody; (2) CESP (*Companhia Energética de São Paulo*) for providing the fish farm facilities; (3) LAQUEFIM (*Laboratório de Aquicultura e Ecofisiologia Marinha*) and LAMEROA (*Laboratório de Metabolismo e Reprodução de Organismos Aquáticos*) team for their help with fish collection; and (4) IB/USP (*Instituto de Biociências, Universidade de São Paulo*) for providing logistics support, infrastructure, and facilities for collection and analysis.

Conflicts of Interest: The authors declare no conflicts of interest.

References

- Honji, R.M.; Caneppele, D.; Hilsdorf, A.W.S.; Moreira, R.G. Threatened fishes of the world: *Steindachneridion parahybae* (Steindachner, 1877) (Siluriformes: Pimelodidae). *Environ. Biol. Fishes* **2009**, *85*, 207–208. [CrossRef]
- IUCN. The IUCN Red List of Threatened Species. Version 2023-1. 2024. Available online: <https://www.iucnredlist.org> (accessed on 21 March 2024).
- Caneppele, D.; Honji, R.M.; Hilsdorf, A.W.S.; Moreira, R.G. Induced spawning of the endangered Neotropical species *Steindachneridion parahybae* (Siluriformes: Pimelodidae). *Neotrop. Ichthyol.* **2009**, *7*, 759–762. [CrossRef]
- Honji, R.M.; Caneppele, D.; Moreira, R.G. Caracterização macroscópica das gônadas durante a reprodução induzida em cativeiro do surubim-do-paíba. *Pesqui. Agropecu. Bras.* **2013**, *48*, 1110–1114. [CrossRef]
- Honji, R.M.; Tolussi, C.E.; Mello, P.H.; Caneppele, D.; Moreira, R.G. Embryonic development and larval stages of *Steindachneridion parahybae* (Siluriformes: Pimelodidae): Implications for the conservation and rearing of this endangered Neotropical species. *Neotrop. Ichthyol.* **2012**, *10*, 313–327. [CrossRef]
- Lopes, T.d.S.; Sanches, E.A.; Okawara, R.Y.; Romagosa, E. Chilling of *Steindachneridion parahybae* (Siluriformes: Pimelodidae) embryos. *Theriogenology* **2015**, *84*, 538–544. [CrossRef]
- Okawara, R.Y.; Sanches, E.A.; Caneppele, D.; Damasceno, D.Z.; Romagosa, E. Ovulation and initial rearing of *Steindachneridion parahybae* (Siluriformes: Pimelodidae) larvae from different accumulated thermal units. *Ichthyol. Res.* **2015**, *62*, 495–503. [CrossRef]
- Tolussi, C.E.; Gomes, A.D.; Ribeiro, C.d.S.; Caneppele, D.; Moreira, R.G.; Honji, R.M. Mobilization of energetic substrates in the endangered catfish *Steindachneridion parahybae* (Siluriformes: Pimelodidae): Changes in annual reproductive cycle in captivity. *Neotrop. Ichthyol.* **2018**, *16*, e170120. [CrossRef]
- Honji, R.M.; Caneppele, D.; Pandolfi, M.; Nostro, F.L.L.; Moreira, R.G. Gonadotropins and growth hormone family characterization in an endangered Siluriform species, *Steindachneridion parahybae* (Pimelodidae): Relationship with annual reproductive cycle and induced spawning in captivity. *Anat. Rec.* **2015**, *298*, 1644–1658. [CrossRef]
- Honji, R.M.; Caneppele, D.; Pandolfi, M.; Nostro, F.L.L.; Moreira, R.G. Characterization of the gonadotropin-releasing hormone system in the Neotropical teleost, *Steindachneridion parahybae* during the annual reproductive cycle in captivity. *Gen. Comp. Endocrinol.* **2019**, *273*, 73–85. [CrossRef]
- Honji, R.M.; Araújo, B.C.; Caneppele, D.; Nostro, F.L.L.; Moreira, R.G. Dynamics of ovarian maturation during the annual reproductive cycle of the endangered fish *Steindachneridion parahybae* (Siluriformes: Pimelodidae) in captivity. *J. Fish Biol.* **2022**, *101*, 55–68. [CrossRef]
- Sanches, E.A.; Marcos, R.M.; Okawara, R.Y.; Caneppele, D.; Bombardelli, R.A.; Romagosa, E. Sperm motility parameters for *Steindachneridion parahybae* based on open-source software. *J. Appl. Ichthyol.* **2013**, *29*, 1114–1122. [CrossRef]
- Sanches, E.A.; Caneppele, D.; Okawara, R.Y.; Damasceno, D.Z.; Bombardelli, R.A.; Romagosa, E. Inseminating dose and water volume applied to the artificial fertilization of *Steindachneridion parahybae* (Steindachner, 1877) (Siluriformes: Pimelodidae): Brazilian endangered fish. *Neotrop. Ichthyol.* **2016**, *14*, e140158. [CrossRef]
- Alix, M.; Kjesbu, O.S.; Anderson, K.C. From gametogenesis to spawning: How climate-driven warming affects teleost reproductive biology. *J. Fish Biol.* **2020**, *97*, 607–632. [CrossRef]
- Servili, A.; Canario, A.V.; Mouchel, O.; Muñoz-Cueto, J.A. Climate change impacts on fish reproduction are mediated at multiple levels of the brain-pituitary-gonad axis. *Gen. Comp. Endocrinol.* **2020**, *291*, 113439. [CrossRef]
- Trudeau, V.L.; Somoza, G.M. Multimodal hypothalamo-hypophysial communication in the vertebrates. *Gen. Comp. Endocrinol.* **2020**, *293*, 113475. [CrossRef]
- Zohar, Y. Fish reproductive biology—Reflecting on five decades of fundamental and translational research. *Gen. Comp. Endocrinol.* **2020**, *300*, 113544. [CrossRef]
- Santhakumar, K. Neuroendocrine regulation of reproduction in fish—Mini review. *Aquac. Fish.* **2024**, *9*, 437–446. [CrossRef]
- Greenwood, A.K.; Wark, A.R.; Fernald, R.D.; Hofmann, H.A. Expression of arginine vasotocin in distinct preoptic regions is associated with dominant and subordinate behaviour in an African cichlid fish. *Proc. R. Soc. B Biol. Sci.* **2008**, *275*, 2393–2402. [CrossRef]
- Sokołowska, E.; Gozdowska, M.; Kulczykowska, E. Nonapeptides arginine vasotocin and isotocin in fishes: Advantage of bioactive molecules measurement. *Front. Mar. Sci.* **2020**, *7*, 610. [CrossRef]
- Pandolfi, M.; Scaia, M.F.; Fernandez, M.P. Sexual dimorphism in aggression: Sex-specific fighting strategies across species. *Front. Behav. Neurosci.* **2021**, *15*, 659615. [CrossRef]
- Silva, A.C.; Pandolfi, M. Vasotocinergic control of agonistic behavior told by Neotropical fishes. *Gen. Comp. Endocrinol.* **2019**, *273*, 67–72. [CrossRef]
- Cavallino, L.; Rincón, L.; Scaia, M.F. Social behaviors as welfare indicators in teleost fish. *Front. Veter-Sci.* **2023**, *10*, 1050510. [CrossRef]
- Godwin, J.; Thompson, R. Nonapeptides and social behavior in fishes. *Horm. Behav.* **2012**, *61*, 230–238. [CrossRef]
- Butler, J.M.; Anselmo, C.M.; Maruska, K.P. Female reproductive state is associated with changes in distinct arginine vasotocin cell types in the preoptic area of *Astatotilapia burtoni*. *J. Comp. Neurol.* **2020**, *529*, 987–1003. [CrossRef]
- Balment, R.; Lu, W.; Weybourne, E.; Warne, J. Arginine vasotocin a key hormone in fish physiology and behaviour: A review with insights from mammalian models. *Gen. Comp. Endocrinol.* **2006**, *147*, 9–16. [CrossRef]

27. Urano, A.; Ando, H. Diversity of the hypothalamo-neurohypophyseal system and its hormonal genes. *Gen. Comp. Endocrinol.* **2011**, *170*, 41–56. [\[CrossRef\]](#)
28. Martos-Sitcha, J.A.; Cádiz, L.; Gozdowska, M.; Kulczykowska, E.; Martínez-Rodríguez, G.; Mancera, J.M. Arginine vasotocin and cortisol co-regulate vasotocinergic, isotocinergic, stress, and thyroid pathways in the Gilthead Sea Bream (*Sparus aurata*). *Front. Physiol.* **2019**, *10*, 261. [\[CrossRef\]](#)
29. Godwin, J. Neuroendocrinology of sexual plasticity in teleost fishes. *Front. Neuroendocr.* **2010**, *31*, 203–216. [\[CrossRef\]](#)
30. Ramallo, M.R.; Grober, M.; Cánepa, M.M.; Morandini, L.; Pandolfi, M. Arginine-vasotocin expression and participation in reproduction and social behavior in males of the cichlid fish *Cichlasoma dimerus*. *Gen. Comp. Endocrinol.* **2012**, *179*, 221–231. [\[CrossRef\]](#)
31. Cunha-Saraiva, F.; Balshine, S.; Gozdowska, M.; Kulczykowska, E.; Wagner, R.H.; Schaedelin, F.C. Parental care and neuropeptide dynamics in a cichlid fish *Neolamprologus caudopunctatus*. *Horm. Behav.* **2019**, *116*, 104576. [\[CrossRef\]](#)
32. Santangelo, N.; Bass, A.H. Individual behavioral and neuronal phenotypes for arginine vasotocin mediated courtship and aggression in a territorial teleost. *Brain, Behav. Evol.* **2010**, *75*, 282–291. [\[CrossRef\]](#) [\[PubMed\]](#)
33. da Silva, M.C.; Canário, A.V.M.; Hubbard, P.C.; Gonçalves, D.M.F. Physiology, endocrinology and chemical communication in aggressive behaviour of fishes. *J. Fish Biol.* **2021**, *98*, 1217–1233. [\[CrossRef\]](#) [\[PubMed\]](#)
34. Foran, C.M.; Bass, A.H. Preoptic GnRH and AVT: Axes for sexual plasticity in teleost fish. *Gen. Comp. Endocrinol.* **1999**, *116*, 141–152. [\[CrossRef\]](#) [\[PubMed\]](#)
35. Goodson, J.L.; Bass, A.H. Forebrain peptide modulation of sexually polymorphic vocal circuitry. *Nature* **2000**, *403*, 769–772. [\[CrossRef\]](#) [\[PubMed\]](#)
36. Goodson, J.L.; Bass, A.H. Social behavior functions and related anatomical characteristics of vasotocin/vasopressin systems in vertebrates. *Brain Res. Rev.* **2001**, *35*, 246–265. [\[CrossRef\]](#) [\[PubMed\]](#)
37. Zanuy, S.; Cerdá-Reverter, J.M.; Muñoz-Cueto, J.A. Cytoarchitectonic study of the brain of a Perciform species, the sea bass (*Dicentrarchus labrax*). I. The telencephalon. *J. Morphol.* **2001**, *247*, 217–228. [\[CrossRef\]](#)
38. Zanuy, S.; Cerdá-Reverter, J.M.; Muñoz-Cueto, J.A. Cytoarchitectonic study of the brain of a Perciform species, the sea bass (*Dicentrarchus labrax*). II. The diencephalon. *J. Morphol.* **2001**, *247*, 229–251. [\[CrossRef\]](#)
39. Cerdá-Reverter, J.M.; Muriach, B.; Zanuy, S.; Muñoz-Cueto, J.A. A cytoarchitectonic study of the brain of a perciform species, the sea bass (*Dicentrarchus labrax*): The midbrain and hindbrain. *Acta Histochem.* **2008**, *110*, 433–450. [\[CrossRef\]](#) [\[PubMed\]](#)
40. Wullimann, M.F.; Rupp, B.; Relchert, H. *Neuroanatomy of Zebrafish Brain: A Topological Atlas*; Birkhaeuser Verlag: Basel, Switzerland, 1996.
41. Zandbergen, M.A.; Kah, O.; Bogerd, J.; Peute, J.; Goos, H.J. Expression and distribution of two gonadotropin-releasing hormone in the catfish brain. *Neuroendocrinology* **1995**, *62*, 571–578. [\[CrossRef\]](#)
42. Dubois, E.A.; Zandbergen, M.A.; Peute, J.; Bogerd, J.; Goos, H.J.T. Development of three distinct GnRH neuron populations expressing two different GnRH forms in the brain of the African catfish (*Clarias gariepinus*). *J. Comp. Neurol.* **2001**, *437*, 308–320. [\[CrossRef\]](#)
43. Ishikawa, Y.; Yoshimoto, M.; Ito, H. A brain atlas of a wild-type inbred strain of the medaka, *Oryzias latipes*. *Fish Biol. J. Medaka* **1999**, *10*, 1–26. [\[CrossRef\]](#)
44. Pandolfi, M.; Pozzi, A.G.; Cánepa, M.; Vissio, P.G.; Shimizu, A.; Maggese, M.C.; Lobo, G. Presence of β -follicle-stimulating hormone and β -luteinizing hormone transcripts in the brain of *Cichlasoma dimerus* (Perciformes: Cichlidae). *Neuroendocrinology* **2008**, *89*, 27–37. [\[CrossRef\]](#) [\[PubMed\]](#)
45. Honji, R.M.; Nóbrega, R.H.; Pandolfi, M.; Shimizu, A.; Borella, M.I.; Moreira, R.G. Immunohistochemical study of pituitary cells in wild and captive *Salminus hilarii* (Characiformes: Characidae) females during the annual reproductive cycle. *SpringerPlus* **2013**, *2*, 460. [\[CrossRef\]](#)
46. Araújo, B.C.; Honji, R.M.; Rombenso, A.N.; de Souza, G.B.; de Mello, P.H.; Hilsdorf, A.W.S.; Moreira, R.G. Influences of different arachidonic acid levels and temperature on the growth performance, fatty acid profile, liver morphology and expression of lipid genes in cobia (*Rachycentron canadum*) juveniles. *Aquaculture* **2019**, *511*, 734245. [\[CrossRef\]](#)
47. de Oliveira, E.F.; Araújo, B.C.; Marques, V.H.; de Mello, P.H.; Moreira, R.G.; Honji, R.M. Influence of docosahexaenoic and eicosapentaenoic acid ratio and temperature on the growth performance, fatty acid profile, and liver morphology of Dusky Grouper (*Epinephelus marginatus*) (Teleostei: Serranidae) juveniles. *Animals* **2023**, *13*, 3212. [\[CrossRef\]](#) [\[PubMed\]](#)
48. Dewan, A.K.; Maruska, K.P.; Tricas, T.C. Arginine vasotocin neuronal phenotypes among congeneric territorial and shoaling reef butterflyfishes: Species, sex and reproductive season comparisons. *J. Neuroendocr.* **2008**, *20*, 1382–1394. [\[CrossRef\]](#) [\[PubMed\]](#)
49. Ohya, T.; Hayashi, S. Vasotocin/isotocin-immunoreactive neurons in the medaka fish brain are sexually dimorphic and their numbers decrease after spawning in the female. *Zool. Sci.* **2006**, *23*, 23–29. [\[CrossRef\]](#) [\[PubMed\]](#)
50. Parhar, I.; Tosaki, H.; Sakuma, Y.; Kobayashi, M. Sex differences in the brain of goldfish: Gonadotropin-releasing hormone and vasotocinergic neurons. *Neuroscience* **2001**, *104*, 1099–1110. [\[CrossRef\]](#)
51. Lema, S.C.; Nevitt, G.A. Variation in vasotocin immunoreactivity in the brain of recently isolated populations of a death valley pupfish, *Cyprinodon nevadensis*. *Gen. Comp. Endocrinol.* **2003**, *135*, 300–309. [\[CrossRef\]](#)
52. Grober, M.S.; George, A.A.; Watkins, K.K.; Carneiro, L.A.; Oliveira, R.F. Forebrain AVT and courtship in a fish with male alternative reproductive tactics. *Brain Res. Bull.* **2002**, *57*, 423–425. [\[CrossRef\]](#)

53. Miranda, J.A.; Oliveira, R.F.; Carneiro, L.A.; Santos, R.S.; Grober, M.S. Neurochemical correlates of male polymorphism and alternative reproductive tactics in the Azorean rock-pool blenny, *Parablennius parvicornis*. *Gen. Comp. Endocrinol.* **2003**, *132*, 183–189. [\[CrossRef\]](#) [\[PubMed\]](#)
54. Larson, E.T.; O'malley, D.M.; Melloni, R.H. Aggression and vasotocin are associated with dominant–subordinate relationships in zebrafish. *Behav. Brain Res.* **2006**, *167*, 94–102. [\[CrossRef\]](#) [\[PubMed\]](#)
55. Iwata, E.; Nagai, Y.; Sasaki, H. Immunohistochemistry of brain arginine vasotocin and isotocin in false clown anemonefish *Amphiprion ocellaris*. *Open Fish Sci. J.* **2010**, *3*, 147–153. [\[CrossRef\]](#)
56. Alonso, F.; Cánepa, M.; Moreira, R.G.; Pandolfi, M. Social and reproductive physiology and behavior of the Neotropical cichlid fish *Cichlasoma dimerus* under laboratory conditions. *Neotrop. Ichthyol.* **2011**, *9*, 559–570. [\[CrossRef\]](#)
57. Xiong, Y.; Wang, X.; Sun, R.; Jiang, Y.; He, Z.; Chen, J.; Li, P.; Mei, J. Administration of arginine vasotocin and modified isotocin improve artificial propagation and post-spawning survival of female yellow catfish. *Aquaculture* **2024**, *587*, 740849. [\[CrossRef\]](#)
58. Maruska, K.P.; Mizobe, M.H.; Tricas, T.C. Sex and seasonal co-variation of arginine vasotocin (AVT) and gonadotropin-releasing hormone (GnRH) neurons in the brain of the halfspotted goby. *Comp. Biochem. Physiol. Part A Mol. Integr. Physiol.* **2007**, *147*, 129–144. [\[CrossRef\]](#) [\[PubMed\]](#)
59. Holmgvist, B.I.; Ekström, P. Hypophysiotrophic systems in the brain of the Atlantic salmon. Neuronal innervation of the pituitary and the origin of pituitary dopamine and nonapeptides identified by means of combined carbocyanine tract tracing and immunocytochemistry. *J. Chem. Neuroanat.* **1995**, *8*, 125–145. [\[CrossRef\]](#) [\[PubMed\]](#)
60. Fox, H.E.; White, S.A.; Kao, M.H.F.; Fernald, R.D. Stress and dominance in a social fish. *J. Neurosci.* **1997**, *17*, 6463–6469. [\[CrossRef\]](#) [\[PubMed\]](#)
61. Pankhurst, N. The endocrinology of stress in fish: An environmental perspective. *Gen. Comp. Endocrinol.* **2011**, *170*, 265–275. [\[CrossRef\]](#)
62. Herrera, M.; Mancera, J.M.; Costas, B. The use of dietary additives in fish stress mitigation: Comparative endocrine and physiological responses. *Front. Endocrinol.* **2019**, *10*, 447. [\[CrossRef\]](#)
63. Morandini, L.; Honji, R.M.; Ramallo, M.R.; Moreira, R.G.; Pandolfi, M. The interrenal gland in males of the cichlid fish *Cichlasoma dimerus*: Relationship with stress and the establishment of social hierarchies. *Gen. Comp. Endocrinol.* **2014**, *195*, 88–98. [\[CrossRef\]](#) [\[PubMed\]](#)
64. Ramallo, M.R.; Birba, A.; Honji, R.M.; Morandini, L.; Moreira, R.G.; Somoza, G.M.; Pandolfi, M. A multidisciplinary study on social status and the relationship between inter-individual variation in hormone levels and agonistic behavior in a Neotropical cichlid fish. *Horm. Behav.* **2015**, *69*, 139–151. [\[CrossRef\]](#) [\[PubMed\]](#)
65. White, S.A.; Fernald, R.D. Changing through doing: Behavioral influences on the brain. *Recent Prog. Horm. Res.* **1997**, *52*, 455. [\[PubMed\]](#)
66. Alward, B.A.; Hilliard, A.T.; York, R.A.; Fernald, R.D. Hormonal regulation of social ascent and temporal patterns of behavior in an African cichlid. *Horm. Behav.* **2019**, *107*, 83–95. [\[CrossRef\]](#) [\[PubMed\]](#)
67. Suarez-Bregua, P.; Guerreiro, P.M.; Rotllant, J. Stress, glucocorticoids and bone: A review from mammals and fish. *Front. Endocrinol.* **2018**, *9*, 526. [\[CrossRef\]](#) [\[PubMed\]](#)
68. Borg, B. Androgens in teleost fishes. *Comp. Biochem. Physiol. Part C Pharmacol. Toxicol. Endocrinol.* **1994**, *109*, 219–245. [\[CrossRef\]](#)
69. Schulz, R.W.; de França, L.R.; Lareyre, J.J.; Le Gac, F.; Chiarini-Garcia, H.; Nobrega, R.H.; Miura, T. Spermatogenesis in fish. *Gen. Comp. Endocrinol.* **2010**, *165*, 390–411. [\[CrossRef\]](#)
70. Damsteegt, E.L.; Thomson-Laing, G.; Wylie, M.J.; Lokman, P.M. Effects of estradiol and 11-ketotestosterone pre-treatment on artificial induction of maturation in silver female shortfinned eels (*Anguilla australis*). *PLoS ONE* **2020**, *15*, e0229391. [\[CrossRef\]](#) [\[PubMed\]](#)
71. Rahdari, A.; Khoshkholgh, M.; Yarmohammadi, M.; Ortiz-Zarragoitia, M.; Lokman, P.M.; Akhavan, S.R.; de Cerio, O.D.; Cancio, I.; Falahatkar, B. The effects of 11-ketotestosterone implants on transcript levels of gonadotropin receptors, and *foxl2* and *dmrt1* genes in the Previtellogenic ovary of cultured beluga (*Huso huso*). *J. Fish Biol.* **2020**, *97*, 374–382. [\[CrossRef\]](#)
72. Alonso, F.; Honji, R.M.; Moreira, R.G.; Pandolfi, M. Dominance hierarchies and social status ascent opportunity: Anticipatory behavioral and physiological adjustments in a Neotropical cichlid fish. *Physiol. Behav.* **2012**, *106*, 612–618. [\[CrossRef\]](#)
73. Ramallo, M.R.; Honji, R.M.; Birba, A.; Morandini, L.; Varela, M.L.; Genovese, G.; Moreira, R.G.; Somoza, G.M.; Pandolfi, M. A game of two? Gene expression analysis of brain (*cyp19a1b*) and gonadal (*cyp19a1a*) aromatase in females of a Neotropical cichlid fish through the parental care period and removal of the offspring. *Gen. Comp. Endocrinol.* **2017**, *252*, 119–129. [\[CrossRef\]](#) [\[PubMed\]](#)
74. Nagahama, Y.; Yamashita, M. Regulation of oocyte maturation in fish. *Dev. Growth Differ.* **2008**, *50*, S195–S219. [\[CrossRef\]](#) [\[PubMed\]](#)
75. Groves, D.; Batten, T. Direct control of the gonadotroph in a teleost, *Poecilia latipinna*. II. Neurohormones and neurotransmitters. *Gen. Comp. Endocrinol.* **1986**, *62*, 315–326. [\[CrossRef\]](#) [\[PubMed\]](#)

Disclaimer/Publisher's Note: The statements, opinions and data contained in all publications are solely those of the individual author(s) and contributor(s) and not of MDPI and/or the editor(s). MDPI and/or the editor(s) disclaim responsibility for any injury to people or property resulting from any ideas, methods, instructions or products referred to in the content.